IN-37
P 35

NASA
Technical
Memorandum

NASA TM-108380

DESIGN OF A WELDED JOINT FOR ROBOTIC, ON-ORBIT ASSEMBLY OF SPACE TRUSSES

By W.K. Rule and F.P. Thomas

Structures and Dynamics Laboratory
Science and Engineering Directorate

October 1992

National Aeronautics and
Space Administration

George C. Marshall Space Flight Center

REPORT DOCUMENTATION PAGE

Form Approved
OMB No. 0704-0188

1. AGENCY USE ONLY (Leave blank)	2. REPORT DATE	3. REPORT TYPE AND DATES COVERED
	October 1992	Technical Memorandum

4. TITLE AND SUBTITLE

Design of a Welded Joint for Robotic, On-Orbit Assembly of Space Structures

5. FUNDING NUMBERS

6. AUTHOR(S)

W.K. Rule* and F.P. Thomas

7. PERFORMING ORGANIZATION NAME(S) AND ADDRESS(ES)

George C. Marshall Space Flight Center
Marshall Space Flight Center, Alabama 35812

8. PERFORMING ORGANIZATION REPORT NUMBER

9. SPONSORING/MONITORING AGENCY NAME(S) AND ADDRESS(ES)

National Aeronautics and Space Administration
Washington, DC 20546

10. SPONSORING/MONITORING AGENCY REPORT NUMBER

NASA TM-108380

11. SUPPLEMENTARY NOTES

Prepared by Structures and Dynamics Laboratory, Science and Engineering Directorate.
*Assistant Professor, Department of Engineering Mechanics, University of Alabama.

12a. DISTRIBUTION/AVAILABILITY STATEMENT

Unclassified—Unlimited

12b. DISTRIBUTION CODE

13. ABSTRACT *(Maximum 200 words)*

A preliminary design for a weldable truss joint for on-orbit assembly of large space structures is described. The joint was designed for ease of assembly, for structural efficiency, and to allow passage of fluid (for active cooling or other purposes) along the member through the joint. The truss members were assumed to consist of graphite/epoxy tubes to which were bonded 2219-T87 aluminum alloy end fittings for welding on-orbit to truss nodes of the same alloy. A modified form of gas tungsten arc welding was assumed to be the welding process. The joint was designed to withstand the thermal and structural loading associated with a 120-ft diameter tetrahedral truss intended as an aerobrake for a mission to Mars.

14. SUBJECT TERMS

Welded Joints, Welding in Space, Robotic Assembly in Space, Large Space Structures

15. NUMBER OF PAGES

35

16. PRICE CODE

NTIS

17. SECURITY CLASSIFICATION OF REPORT	18. SECURITY CLASSIFICATION OF THIS PAGE	19. SECURITY CLASSIFICATION OF ABSTRACT	20. LIMITATION OF ABSTRACT
Unclassified	Unclassified	Unclassified	Unlimited

TABLE OF CONTENTS

LIST OF ILLUSTRATIONS

TECHNICAL MEMORANDUM

DESIGN OF A WELDED JOINT FOR ROBOTIC, ON-ORBIT ASSEMBLY OF SPACE TRUSSES

I. INTRODUCTION

In the future, some spacecraft will be so large that they must be assembled on-orbit.[1–4] These spacecraft will be used for such tasks as manned missions to Mars or will be used as orbiting platforms for monitoring the Earth or observing the universe. Large spacecraft will probably consist of planar truss structures to which will be attached special-purpose, self-contained modules. The modules will most likely be taken to orbit fully outfitted and ready for use in heavy-lift launch vehicles. The truss members will also similarly be taken to orbit, but mostly unassembled. The truss structures will need to be assembled robotically because of the high costs and risks of extravehicular activities (EVA's). Some missions will involve very large loads. For instance, the truss structure supporting an aerobrake heat shield will experience up to 6 g's of deceleration during entry into the Martian atmosphere.[5]

To date, very few structures of any kind have been constructed in space. Two relatively simple trusses were assembled in the space shuttle bay in 1985.[6]

The development of a design for a welded joint for an on-orbit, robotic-truss assembly is described here. Mechanical joints for this application have been considered previously.[7 8] Welded joints have the advantage of allowing the truss members to carry fluids for active cooling or other purposes. Welded joints can be made more efficient structurally than mechanical joints. Also, welded joints require little maintenance (will not shake loose) and have no slop which would cause the structure to shudder under load reversal. The disadvantages of welded joints are that a more sophisticated assembly robot is required, weld flaws may be difficult to detect on-orbit, the welding process is hazardous, welding consumes a significant amount of power, and welding introduces contamination to the environment. In addition, welded joints provide less structural damping than do mechanical joints.

Welding on-orbit was first investigated aboard a Soyuz-6 mission in 1969 and then during a *Skylab* electron beam welding experiment in 1973.[9 10] A hand-held, electron-beam welding apparatus is currently being prepared for use on the *MIR* space station.[11] Presently, Marshall Space Flight Center (MSFC) is evaluating processes appropriate for on-orbit welding.[12] A low-gravity environment has been found to have very minor effects on the welding processes appropriate for this application. This finding is based on tests run on-orbit as well as low-gravity environments achieved by flying aircraft in parabolic trajectories. In fact, low gravity can make welding easier since the flow of the molten metal is dictated by surface tension effects undisturbed by gravitational forces.[12]

It appears that a modified form of gas tungsten arc welding (GTAW) will be most appropriate for welding together structures on-orbit.[12] The process has been modified to work in a vacuum by providing gas to the arc zone by means of a hollow tungsten electrode with special shielding. A commercial tube-welding head has been successfully modified for use on-orbit with a gas leakage rate of approximately 2.5 L/min.[12]

To develop as realistic a joint as possible, a specific truss structure was selected on which to base the design. The structure considered was based on the 120-ft diameter aerobrake tetrahedral truss structure described in references 5, 7, and 8. Structural characteristics of tetrahedral trusses are also discussed in reference 13. The truss members were assumed to consist of graphite/epoxy tubes. Also, it was assumed that the nodes were constructed of 2219-T87 aluminum alloy. The magnitude of the member load assumed for design purposes was 100 kips.

No manufacturing process or robot is perfect, so it is anticipated that the truss members will be slightly too long or short after welding. These member misfits will be randomly distributed throughout the structure and will lock in member forces and distort the truss before service loads are applied. This effect is considered in section II. These misfits will also cause the nodes of a partially assembled truss to move away from their ideal positions. Thus, the assembly robot will be required to pull the nodes together or push them apart while assembling the last few members of the truss. The force required to do this is discussed in section III. Both of these effects need to be considered while developing a joint design. Mechanical details of the welded joint design are given in section IV. Peak temperatures in the vicinity of the fusion line of the weld are investigated in section V. Conclusions derived during the course of this study are listed in section VI.

II. MEMBER FORCES GENERATED BY RANDOM MEMBER MISFITS

A structural configuration must be selected before a welded joint can be designed. Here, an approximately 120-ft diameter tetrahedral truss structure (fig. 1) was considered based on the aerobrake structure of reference 7. The 660 members of the tetrahedral truss were all 12.56-ft long and consisted of identical graphite/epoxy tubes (elastic modulus = 10.5E6 lb/in^2, shear modulus = 4.0E6 lb/in^2, Poisson's ratio = 0.33, outside diameter = 5 in, wall thickness = 0.375 in). The truss was 10.25-ft deep in accordance with the geometric properties of a tetrahedron.

No manufacturing or assembly process is absolutely accurate. Thus, after being welded into the truss, the members will tend to be slightly too long or short. These randomly distributed misfits will lock in member forces before service loads are applied. The misfits will also distort the truss to some degree. Before a joint can be designed, some measure of an acceptable misfit must be determined which will dictate the accuracy required of the robot and the joint configuration. Member misfits will be randomly distributed, so peak member forces can only be determined in a statistical sense. The structure was analyzed 50 times with different randomly generated sets of member misfits, and the mean and standard deviations of the peak member force magnitudes were calculated from these results. The technique used to perform these calculations will now be described.

The MSC/pal 2 (version 3.0) finite-element program was used to perform the calculations.[14] A partial listing of the model input deck is shown in figure 2. A full listing of the nodal coordinates and the nodal connectivities of the elements is provided in appendices A and B, respectively. The model consisted of tubular-beam elements rigidly connected at the nodes—a frame structure. Rigid nodal connections were assumed because the joints will be welded. However, since all loads will be applied through the nodes, the structure will behave very much like a truss.

Figure 2 indicates that all the displacement components of node 161, which is at the center of the top plane of the truss, were made to equal zero. This was done to remove the rigid-body displacement modes, thus making the stiffness matrix nonsingular (invertable). Node 161 was arbitrarily selected; any

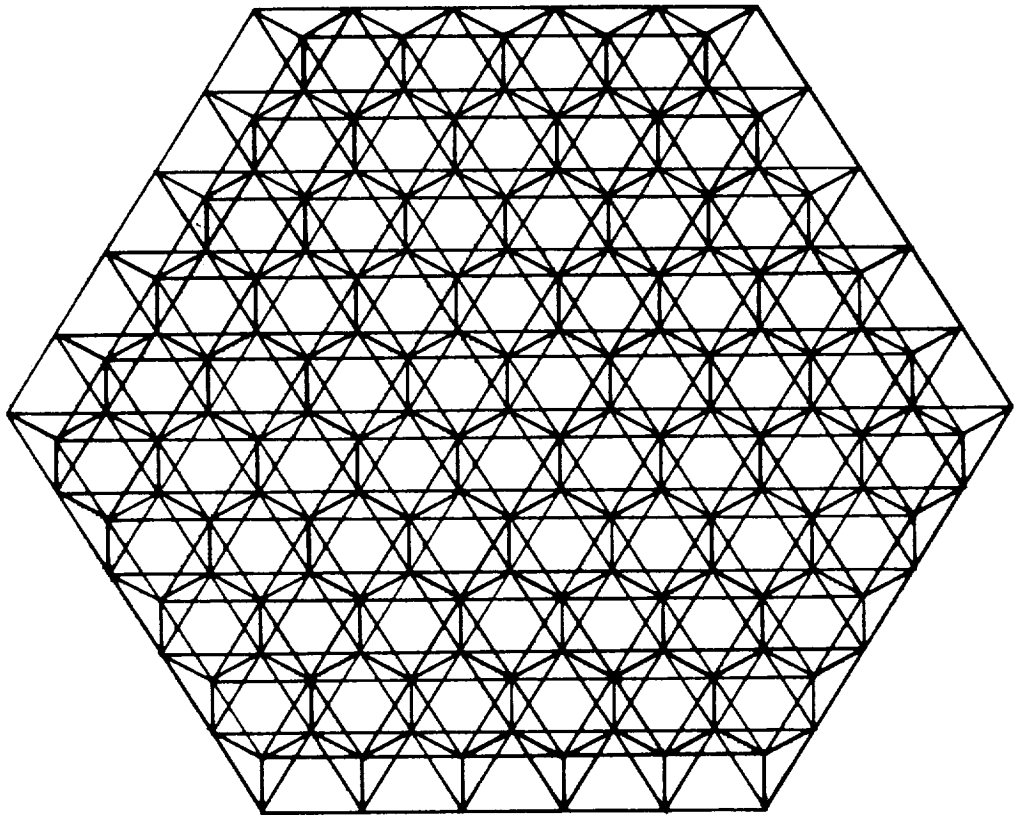

(a) Top View

(b) Side View

Figure 1. Structural configuration of the undeformed truss.

other node could have been similarly fixed with no effect on the calculated member forces. This is because the nodal loads produced by the member misfits are self-equilibrating, as will be discussed.

The member misfits were treated in the following manner. First, a different misfit for each member was calculated using a random number generator. The random number generator was set up to produce values varying between minus and plus a specified maximum misfit magnitude. Then, the force required to make the member (with random misfit) fit between its nodes was calculated using elementary strength of materials theory

$$F_i = \frac{-EAD_i}{L} \quad , \tag{1}$$

where F_i is the force in the ith member, E is the elastic modulus, A is the cross-sectional area, D_i is the misfit in the ith member, and L is the member length. Note that if D_i is negative (member a little too short), then equation (1) indicates that F_i will be positive (tensile) since the member would have to be stretched to fit between its nodes. Similarly, a positive D_i will produce a compressive (negative) force in

```
TITLE STRUCTURE MODEL FILE
NODAL POINT LOCATIONS 1
161 0,0,10.25
163 12.56,0,10.25
193 6.28,10.88,10.25

.
.
.

106 43.95,-25.38,0
138 50.23,-14.5,0
170 56.51,-3.63,0

MATERIAL PROPERTIES 1.512E9,5.76E8,0,0.33,8.352E6
BEAM TYPE 3,0.4167,0.3542
DO CONNECT 31 32 THROUGH 42 43 STEP 1 1
DO CONNECT 61 62 THROUGH 74 75 STEP 1 1
DO CONNECT 91 92 THROUGH 106 107 STEP 1 1

.
.
.

DO CONNECT 92 124 THROUGH 284 316 STEP 32 32
DO CONNECT 122 154 THROUGH 282 314 STEP 32 32
DO CONNECT 152 184 THROUGH 280 312 STEP 32 32
ZERO 1
ALL 161

END DEFINITION
```

Figure 2. MSC/pal 2 finite-element model input deck for the tetrahedral truss.

a member. These F_i were considered to be initial forces in the members. With these initial forces applied, all members will be the same length and will fit together perfectly to produce the undistorted truss of figure 1. Thus, this initial member force technique allows the same undistorted finite-element model to be used for all sets of member misfit analyses.

The initial member forces will produce forces on the nodes. A member with an initial tensile load will tend to pull its nodes together. Similarly, a compressively loaded member will tend to push its nodes apart. Since the member forces can be calculated from equation (1), the nodal loads associated with member forces are also known and can be applied to the nodes in the form of a load vector. The nodal loads produced by the internal force in each member were broken down into components along the global cartesian coordinate directions (based on the orientation of the member) and summed up (for all members) to produce a global nodal load vector. Note that a member will push or pull one way on one node but the opposite way on its other node—a self-equilibrating force set. A typical MSC/pal 2 load file of misfit-generated nodal loads is shown in figure 3.

The analysis procedure can be summarized as follows. Random member misfits are generated, and the associated initial member forces are calculated and stored in a file. Nodal loads due to the initial member forces are calculated and summed up to form a global nodal load vector. The load vector is applied to the structure, and the finite-element program is run to calculate a set of intermediate member loads. To save solution time here, the stiffness matrix was inverted (decomposed) only once, and the restart mode of MSC/pal 2 was used for all subsequent runs. Finally, the initial member loads are added to the intermediate member loads to produce a set of final member loads. The two Microsoft QuickBASIC programs that were written to perform these calculations will now be described.

```
TITLE MEMBER LENGTH ERROR LOAD FILE

FORCES AND MOMENTS APPLIED 0
FX   1  -230442.5204966329
FY   1   53184.79766821611
FZ   1   49436.58426652521
FX   3  -158863.1236084707
FY   3  -270611.7564973687
FZ   3  -203426.5088492376
FX   5  -77143.89459794664
FY   5   48554.34908752082
FZ   5  -190155.6006866425
FX   7  -65203.79829002415
FY   7  -77442.82862363869
FZ   7   262003.1117336018
FX   9   334861.5685711871

.
.
.

FX  319   39670.97931474186
FY  319  -396517.7200944773
FZ  319   303580.2824678487
FX  320   99311.72126063828
FY  320   386502.2201876945
FZ  320  -254415.5649100334
FX  321  -270827.0943719279
FY  321  -192052.8781665579
FZ  321  -83481.81538990338

SOLVE
QUIT
END
```

Figure 3. Typical MSC/pal 2 random-member misfit-loading input deck.

Program CALCMSFT (CALCulate MiSFiT) is listed in appendix C, and it performs the following tasks. First, it reads in files containing listings of the nodal coordinates and nodal connectivities of the elements. These files are generated by the "TABULAR LISTS" function of the VIEW2 program of MSC/pal 2. Then, CALCMSFT reads in the maximum length error (misfit) magnitude, the elastic modulus, the member outside diameter, and the member inside diameter. This information is used to calculate the misfit-induced initial member forces (which are stored in a file for later use) and the nodal loads resulting from these initial member forces. CALCMSFT then appends these nodal loads to a nodal load "stub" file to form a load file appropriate for input to the STAT2 program of MSC/pal 2. Here the stub file simply contains the run title and a blank line. Program STAT2 is then run (in restart mode for all runs except the first) to calculate a set of intermediate member forces.

The other program written to investigate the member force effects of misfits is called GETFORCE, and it is listed in appendix D. First, this program reads in the results output file produced by the STAT2 program of MSC/pal 2. The following STAT2 output options are used when generating the output file: no applied forces, no external forces, no displacements, full-element analysis, calculate average nodal stresses, and process all elements. GETFORCE searches through the results output file and stores the member "intermediate" forces in an array. GETFORCE adds the initial member forces (previously stored by the CALCMSFT program) to the intermediate member forces to produce a set of final member forces. GETFORCE then searches through the array of final member forces to find the largest magnitude of member force. Finally, GETFORCE writes this information and all final member forces to a file.

Fifty sets of random member misfits were generated and the corresponding final member forces calculated. The member force results were scaled and nondimensionalized by dividing by the magnitude of member force that would be generated if the maximum misfit (the value input to program CALCMSFT) was applied to a member, and then this member was stretched or compressed so that it returned to its nominal length. Thus, the scaling factor can be calculated from the magnitude of the F_i given by equation (1) with the D_i set to the maximum member misfit magnitude. In other words, the scaling factor is equal to the magnitude of the largest possible misfit force for the case of a structure consisting of a single member placed between two rigid walls. This scaling technique allows the results of this study to be applied to other similar trusses.

The average maximum (scaled) member force for the 50 runs was 1.04 with a standard deviation of 0.22. These two values can be used to make a prediction of the maximum misfit-generated member force likely to occur for a given level of certainty. For instance, the maximum member force magnitude will be less than the mean plus two standard deviations (1.04+2(0.22) = 1.5) with a certainty of 97 percent. Accordingly, the peak member force with a 97-percent level of certainty can be estimated as follows:

Step 1: Estimate the maximum member misfit. This will be due to two sources: the tolerance on the manufacturing process used to fabricate the member and associated nodes on Earth, and the tolerance on the robotic assembly of the member on-orbit. These numbers are difficult to estimate. The tighter the tolerance, the higher the cost of the structure. Suppose that these tolerances can be economically held to 0.01 inch in a mass production environment. Thus, the maximum member misfit will be $D_{max} = 0.01+0.01 = 0.02$ inch.

Step 2: Determine the scaling force, F_s. From equation (1):

$$F_s = \frac{EAD_{max}}{L} = \frac{(10.5E6)(5.45)(0.02)}{(150.7)} = 7.6 \text{ kips} \ .$$

Step 3: Multiply the scaling force by the 97-percent force multiplier to calculate the predicted maximum member force, F_{max}:

$$F_{max} = 1.5F_s = (1.5)(7.6) = 11.4 \text{ kips} \ .$$

F_{max} could be a tensile or a compressive force. Note that F_{max} amounts to a significant portion of the member design load of 100 kips.

Besides generating member forces, random member misfits will also distort the structure. The distortion (greatly exaggerated) of a typical member misfit analysis is shown in figure 4. This type of distortion may cause problems for truss structures supporting equipment with fine pointing requirements or the heat shield associated with aerobrake structures.[15]

Member misfits will also cause the nodes of a partially assembled structure to move apart or closer together. Thus, the assembly robot will be required to exert forces on adjacent nodes while assembling a member. The magnitude of these forces will impact the design of both the robot and the joint. This effect is considered in the next section.

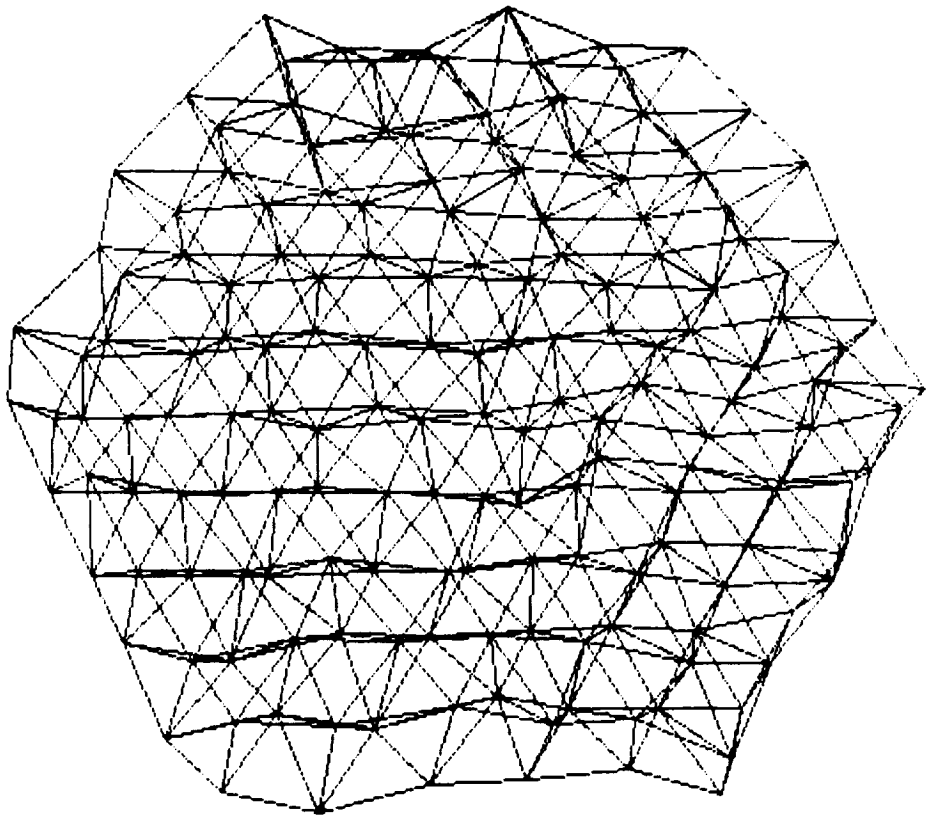

(a) Top View

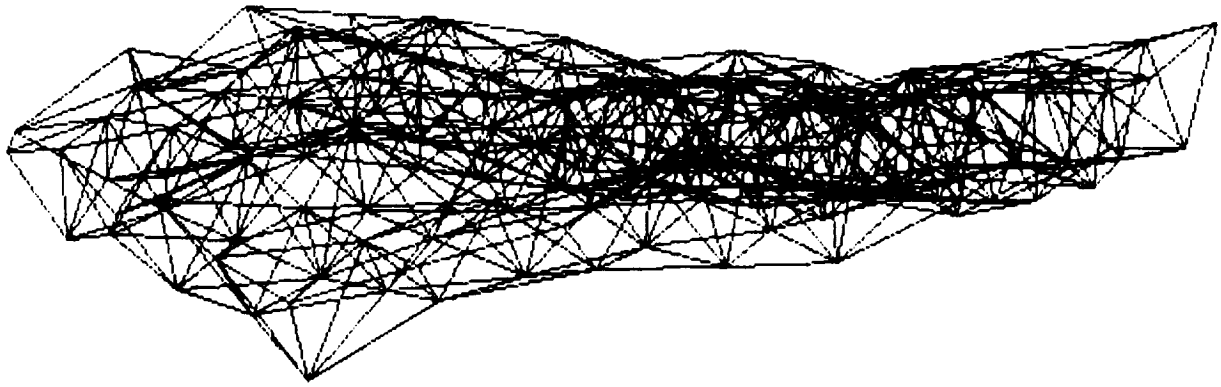

(b) Side View

Figure 4. Typical deformed shape of the tetrahedral truss due to random member misfit loading.

III. NODE SEPARATION INDUCED BY RANDOM MEMBER MISFITS

The effect of member misfits, in terms of member forces locked in, was discussed in the previous section. Here, the effect of member misfits on relative nodal displacements of a partially assembled truss structure is considered. Misfit-induced member forces will cause the truss to distort and, thus, will cause pairs of nodes to move closer together or farther apart. These relative nodal displacements will have to

be corrected by the robot during the assembly process. As more members are assembled, relative nodal displacements will tend to increase since there are more member misfits to cause distortion. Thus, the robot will have to make the largest relative nodal displacement corrections while assembling the last few members of the truss.

To correct for these misfit-induced relative nodal displacements, the robot will be required to push or pull on pairs of nodes. The magnitude of force required to make these corrections must be estimated because it affects the design of both the robot and the joint. The correction force can only be estimated in a statistical sense since the member misfits are randomly distributed.

To be conservative, the correction force required while assembling the last member of the structure was considered. It was assumed that the structure will be assembled from one edge through to a far edge, so the last member would be an edge member. Accordingly, for this relative nodal displacement correction force study, an edge member was removed from the structure described in the previous section. The edge member removed was connected to nodes 318 and 320, as shown in figure 5. Nodes 318 and 320 are on a line parallel to the global x-axis.

The analysis procedure involved the following steps. First, program CALCMSFT (described in the previous section) was run to generate a set of random misfit-induced nodal forces for the structure with the edge member removed. These loads were then input to the STAT2 program of MSC/pal, and the nodal displacements due to these forces were calculated. An output file was created by STAT2 containing these displacement results. The following STAT2 output options were used while generating the output file: no applied forces, no external forces, full displacement components, and no element output. Program GETDISPL was then run to read the displacements of the STAT2 output file and to calculate the relative displacement between nodes 318 and 320. Program GETDISPL was written in Microsoft QuickBASIC and is listed in appendix E.

This analysis procedure was repeated with 50 sets of random member misfits so that the mean and the standard deviation of the misfit-induced relative displacement between nodes 318 and 320 could be calculated. Note that STAT2 was run in the restart mode for all except the first run to save computational time. Nodes 318 and 320 form a line parallel to the global x-axis. It can be shown that to a first-order level of accuracy the change in distance (relative displacement) between nodes 318 and 320 is the algebraic difference between their respective x-displacements.

The calculated results were scaled and nondimensionalized by dividing the mean and standard deviation by the maximum member misfit magnitude, which was an input to program CALCMSFT. This scaling conveniently allows the results obtained to be used for any assumed maximum member misfit for the particular truss under consideration here, and the results can also be applied to other similar trusses. The scaled mean and standard deviation of the relative displacement between nodes 318 and 320, as determined by the 50 simulations, were 1.00 and 0.72, respectively. Thus, to a 97-percent level of certainty, the scaled relative displacement between nodes 318 and 320 will be less than $1.00+2(0.72) = 2.44$.

The spring stiffness associated with pulling nodes 318 and 320 together or pushing them apart was determined in the following manner. A unit load was applied to node 318 in the direction of node 320 (parallel to x-axis). Another unit load was applied to node 320 in the direction of node 319. Program STAT2 was then run to calculate the relative x-displacement between these two nodes due to the unit loads. Note that the member between nodes 318 and 320 was removed during this process. The magnitude of forces applied (unity) divided by the relative x-displacement gives the node-to-node spring

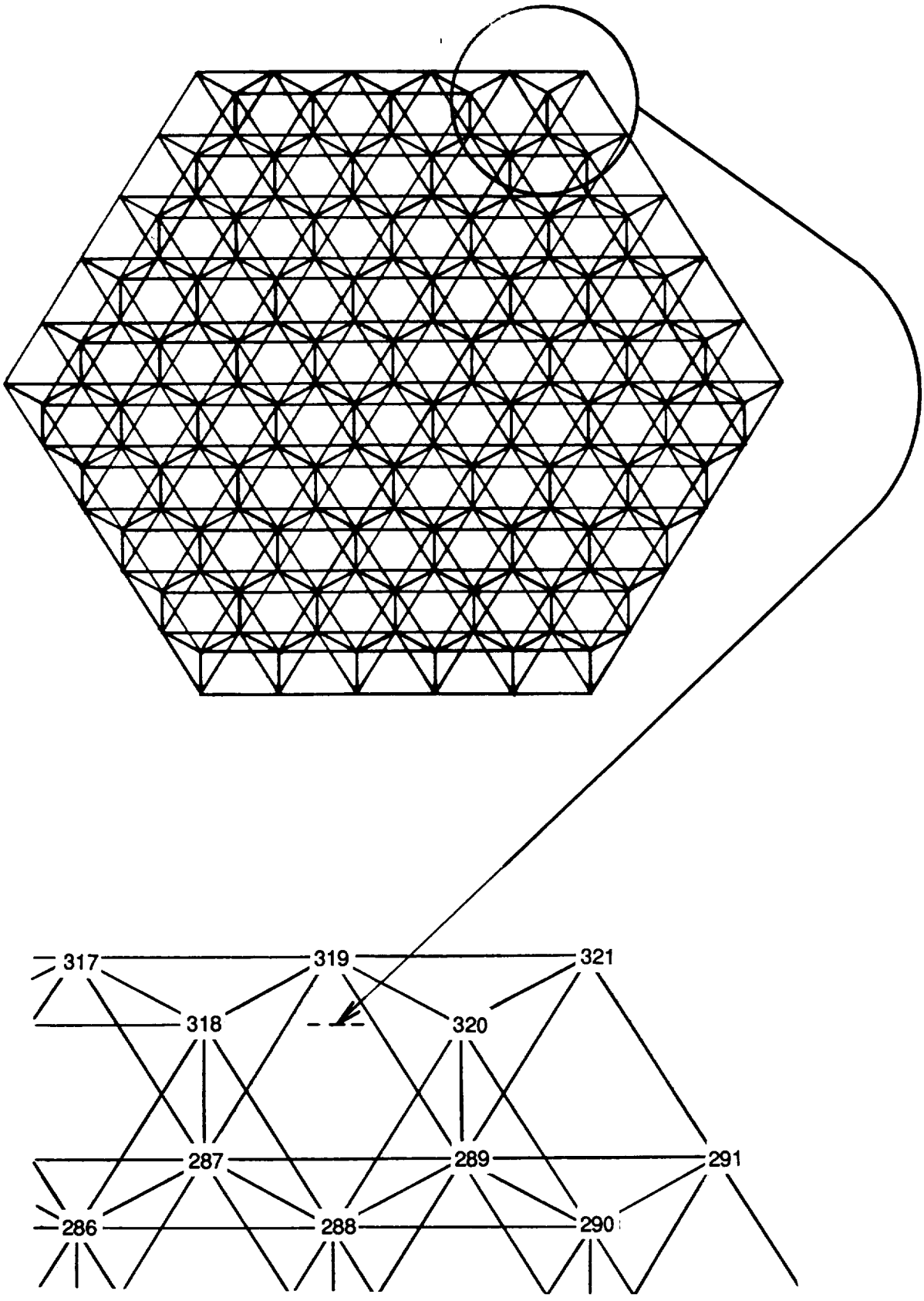

Figure 5. Location of member removed from structure to calculate the relative displacement between nodes 318 and 320 due to member misfits.

constant, k_n. Of course k_n would vary throughout the structure depending on which pair of nodes was considered. However, the k_n associated with nodes 318 and 320 is representative of the structure as a whole. The calculated 318 to 320 k_n was 7.76E4 lb/in. This amounts to about 20 percent of the spring stiffness of an individual member. The robot must push or pull against this "spring" while attempting to correct for member misfit-induced relative nodal displacements.

The peak force that a robot will likely have to exert with a 97-percent level of certainty can be estimated as follows:

Step 1: Estimate the maximum member misfit. This was discussed previously, and a value of D_{max} of 0.02 in was suggested.

Step 2: Calculate the maximum relative joint displacement, $D_{max,joint}$:

$$D_{max,joint} = (\text{scaled displacement multiplier, 97-percent level of certainty})*D_{max}$$

$$= (2.44)(0.02) = 4.88\text{E-}2 \text{ in.}$$

Step 3: Calculate the maximum force likely (97-percent level of certainty) to be required of the robot to correct for member misfit-induced relative nodal displacements, $F_{max,robot}$:

$$F_{max,robot} = k_n D_{max,joint} = (7.76\text{E}4)(4.88\text{E}{-2}) = 3.8 \text{ kips (either push or pull)} .$$

This analysis has shown that the assembly robot must be capable of pulling or pushing with a relatively large force while attempting to correct for member misfit-induced relative nodal displacements.

In the next section, the details of the design of the welded joint will be considered.

IV. DESIGN OF THE WELDED JOINT

A. Design Philosophy

The trusses under consideration here will be robotically assembled on-orbit. This makes it imperative that the truss members and joints be "designed for assembly." The design should be such that the robot can: easily transport the member from the pallet it was taken into orbit on to the appropriate position on the truss; insert the member between the nodes; correct the node positions for member misfit errors; and then weld the member into position.

The members and joints must also be light and able to be densely packed together for efficient transport to orbit, a major cost driver. A light design is also necessary to control inertial forces while in service. The joint components must be relatively easy to produce so that manufacturing costs will not be excessive. The joint design must provide a seal so that fluids may be pumped throughout the members of the truss. Based on prior studies,[7] it was assumed that the joint must be capable of carrying 100 kips, and that the members consist of graphite/epoxy tubes of circular cross section (5-in outside diameter, 0.375-in wall thickness).

A major difficulty with the joint design was allowing for the member to be connected to the nozzles of two nodes that had already been welded into position. This could be handled in two ways. A member could be made precisely the correct length so that it could be positioned between the node nozzles (without being inserted) and then welded into place. This approach has two major drawbacks: the joint configuration provides no alignment assistance to the robot, and joint gap control would be difficult. Alternatively, one half of the member could be designed to telescope into the other as shown in figure 6. This would allow a member to be shortened (telescoped), placed between the nodes, and then extended so that its ends would fit inside the nozzles of the nodes (fig. 7). This provides for very accurate alignment of the joints and complete control of the weld joint gap. The joint overlap shown in figure 7 is tapered to facilitate insertion into the nozzle of the node. When the joint has been fully made up, the joint overlap will be snug against the inside surface of the nozzle of the node, and the joint will be temporarily held together by the friction provided by the compressed O-ring (fig. 7). The telescoping action allows for very compact shipment to orbit. A disadvantage of the telescoped member approach is that three weld joints will now have to be made (at each end and at the sliding joint in the middle) instead of the two required for the nontelescoped design. However, it appears that the telescoped design will make it easier for the robot to assemble and weld the structure; therefore, the telescoped design was selected for further study.

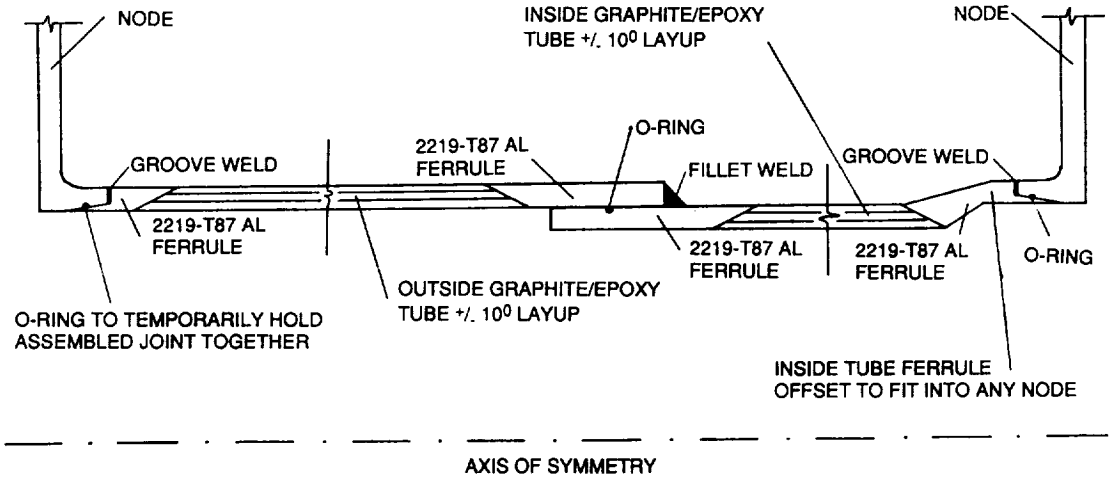

Figure 6. Truss member telescoping design concept.

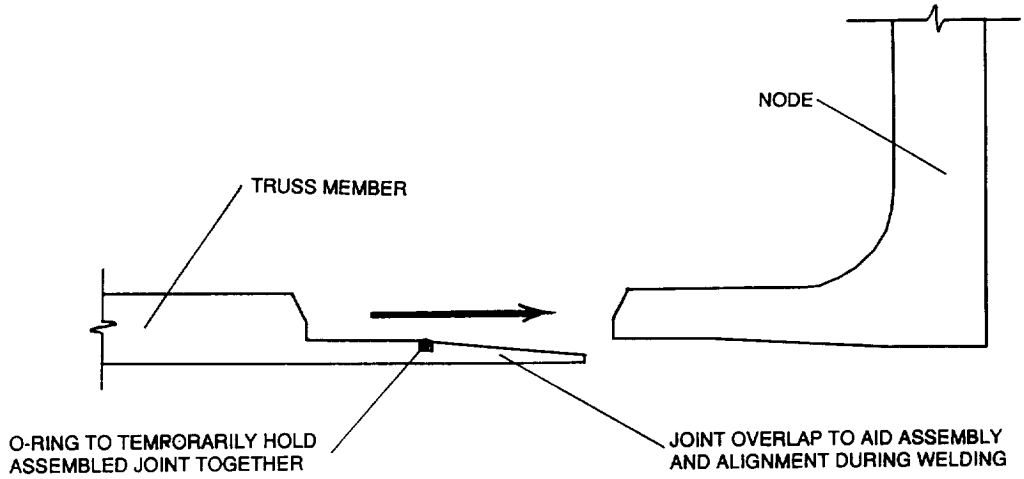

Figure 7. Joint overlap to aid assembly and alignment during welding.

B. Finite Element Analysis of the Aluminum Components of the Welded Joint

A preliminary analysis of the joint using an isotropic finite-element model without thermal loading was conducted using the MSC/pal 2 program. The MSC/pal 2 program can make no provision for anisotropic material properties; therefore, a detailed analysis of the composite material portion of the joint or a thermal loading analysis could not be performed using this program. These effects are discussed in the next section. The analysis described in this section was undertaken to develop an initial concept for the joint design such that the stresses in the aluminum components (both parent and weld metal) were less than the yield stress when factored loads were applied. A listing of the MSC/pal 2 input deck is given in appendix F, and the finite element mesh and joint dimensions are displayed in figure 8. Axisymmetric elements were used in the analysis.

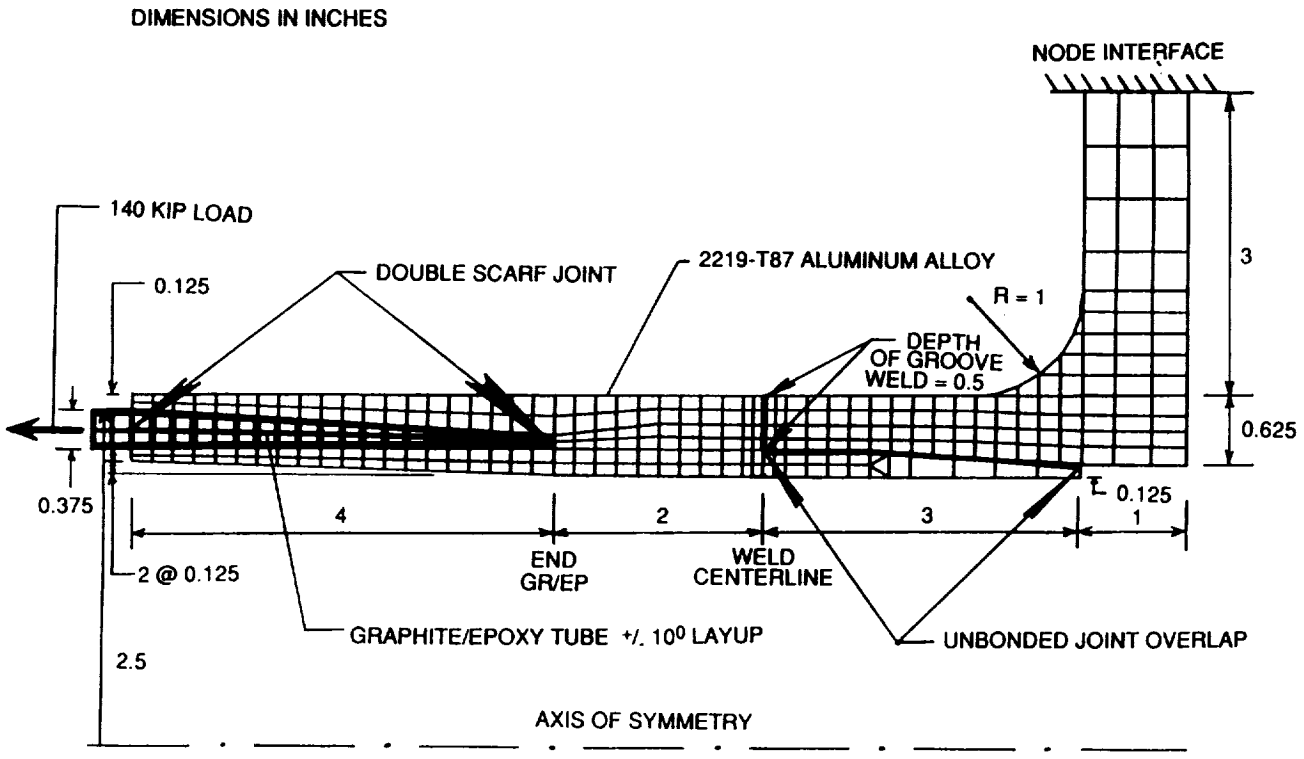

Figure 8. MSC/pal 2 finite-element model of preliminary joint design.

As shown in figure 8, the part of the node that the truss member ferrule was welded to was assumed to consist of a nozzle similar to that found in pressure vessels. A design of this nature allows for the easy passage of fluid along the truss member and into the node. This configuration also provides for a very simple and clean design of both the member ferrule, the weld, and the node. However, the nozzle approach is not very efficient structurally since the load path must change abruptly as axial loads run from the member into the node. This produces large bending stresses in the node fitting (fig. 9). Thus, generous fillets and relatively thick components will be required for the design of the node. Figure 8 shows that the node component was rigidly fixed at a somewhat arbitrary radial distance of 3 in from the outer wall of the member. A more accurate value for the effective support distance can be obtained when a design for the node becomes available. Figure 9 demonstrates that with the factored axial load applied (140 kips), the maximum Von Mises stresses in the node portion of the joint and in the ferrule outside of the weld are held to less than the 51 ksi yield stress of 2219-T87 aluminum.[16]

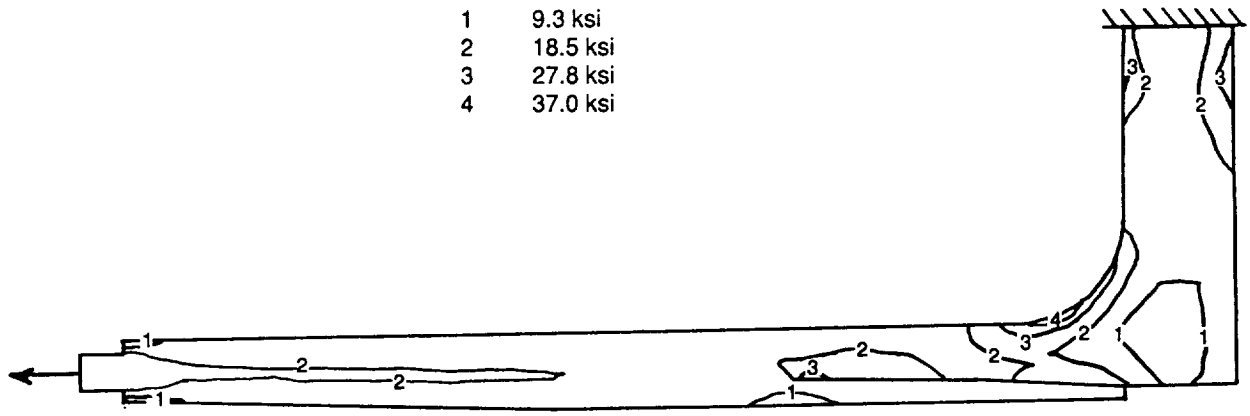

Figure 9. Von Mises stress contours in preliminary joint design.

As was illustrated in figure 7, a joint overlap will be provided to aid assembly and to provide alignment during welding. The geometric discontinuity associated with the joint overlap produces a small stress concentration at the root of the weld (fig. 9). This stress concentration dictates that a GTAW groove weld 0.5-in deep is required to keep the Von Mises stress level within the heat affected zone (HAZ) to less than the weld metal yield stress of 26 ksi.[17]

Figure 8 shows a double scarf joint for the composite strut-aluminum ferrule connection. This joint was subsequently redesigned due to concerns about manufacturability and thermal loading capacity. The redesigned joint is the subject of the next section. Redesigning the composite material-aluminum joint will not significantly affect the stresses in the vicinity of the weld.

C. Design of the Connection Between the Graphite/Epoxy Tube and the Aluminum Joint

For many applications, the ideal design of the graphite/epoxy strut will consist of laying up the fibers such that they are oriented at ±10° with respect to the axis of the member.[5] This layup will provide for high stiffness and strength parallel to the axis of the member, along with a slightly negative axial coefficient of thermal expansion. The slightly negative coefficient of thermal expansion of the struts, coupled with the relatively large positive coefficient of thermal expansion of the aluminum fittings can produce members with a net axial coefficient of thermal expansion of zero. This is highly desirable in spacecraft since it prevents temperature changes from causing structural distortions.

However, a ±10° layup will create some problems, especially in applications where the composite material must be attached to a metallic component in an environment where there will be large temperature changes, as is the case here. In this study, it was assumed that during the mission temperature variations as large as ±250 °F could occur. The primary difficulty with this type of joint is that the coefficient of thermal expansion of the composite in the circumferential direction is five times that of the aluminum.

The design illustrated in figure 10 was investigated as a means of coping with the large differences in the anisotropic coefficients of thermal expansion of the graphite/epoxy material and that of the aluminum. This design incorporates a joint reinforcing ring of graphite epoxy with a quasi-isotropic ±45° layup. As indicated in figure 10, this reinforcing ring has coefficients of thermal expansion which

are roughly midway between those of the strut and the ferrule. In addition, the reinforcing ring has relatively low elastic moduli. Thus, the reinforcing ring is intended to act as a compliant structure to help smooth the transition from the ±10° layup graphite/epoxy strut to the aluminum ferrule.

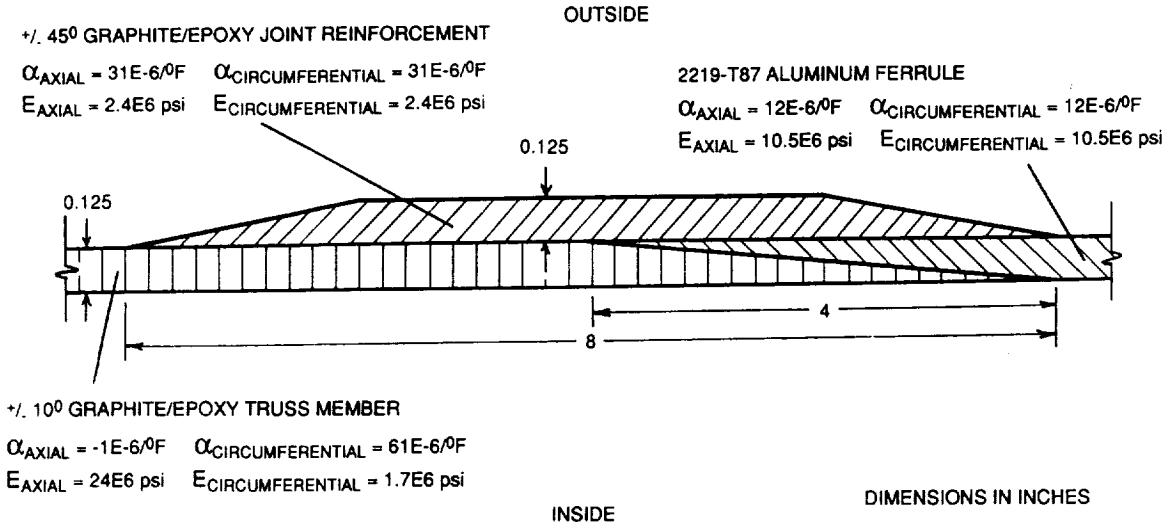

Figure 10. Drawing of composite material strut-aluminum end fitting joint.

This design would be fabricated by first machining down the ends of the graphite/epoxy truss member and that of the aluminum ferrule in the form of opposing 4-in long linear tapers. There is no difficulty machining graphite/epoxy materials with tungsten-carbide tipped tools.[18] The graphite/epoxy and aluminum components would then be bonded together using an epoxy adhesive. The assumed maximum design temperature of the adhesive was 300 °F. At this temperature, a typical epoxy adhesive has an ultimate shear strength of approximately 1.3 ksi.[19] After the epoxy adhesive has cured and the outside surface of the tube in the vicinity of the joint has been cleaned, the ring of joint reinforcement is applied in the form of a prepreg tape or other convenient means. Care should be taken to obtain a good bond between the reinforcing ring and the tube. After the reinforcing ring has cured, the edges of the ring should be machined down to form a linear taper (fig. 10). Tapered joints tend to produce a uniform shear stress distribution in the bond line.[18]

The joint of figure 10 was analyzed using the COSMOS/M finite element program[20] which, unlike the MSC/pal 2 program, has some capability to treat anisotropic material behavior. The COSMOS/M input deck used to model the joint is listed in appendix G. The model consisted of 593 nodes and 483 axisymmetric elements. The material properties used in the model were as follows (x-axis is radial coordinate, y-axis runs along axis of symmetry):

1. 2219-T87 Aluminum

$$E = 10.5\text{E6 lb/in}^2,\ \nu = 0.33,\ \alpha = 12\text{E-6/°F},\ \sigma_{yield} = 51\text{ ksi}.$$

2. ±10° Layup Graphite/Epoxy

$$E_x = 24\text{E6 lb/in}^2,\ E_y = 1.7\text{E6 lb/in}^2,\ E_z = 1.7\text{E6 lb/in}^2,\ \nu_{xy} = 0.3,\ \nu_{xz} = 0.3,$$

$$\nu_{yz} = 0.3,\ G_{xy} = 0.65\text{E6 lb/in}^2,\ \alpha_x = -1\text{E–6/°F},\ \alpha_y = 63\text{E–6/°F},\ \alpha_x = 61\text{E–6/°F},\ \sigma_{y,max} = 42\text{ ksi}.$$

3. ±45° Layup Graphite/Epoxy

$$E_x = 2.4\text{E}6\ \text{lb/in}^2,\ E_y = 1.7\text{E}6\ \text{lb/in}^2,\ E_z = 2.4\text{E}6\ \text{lb/in}^2,\ \nu_{xy} = 0.3,\ \nu_{xz} = 0.3,$$

$$\nu_{yz} = 0.3,\ G_{xy} = 0.65\text{E}6\ \text{lb/in}^2,\ \alpha_x = 31\text{E}{-6}/°\text{F},\ \alpha_y = 63\text{E}{-6}/°\text{F},\ \alpha_z = 31\text{E}{-6}/°\text{F},\ \sigma_{y,\max} = 7\ \text{ksi}\ .$$

These values are meant to represent typical high-modulus graphite/epoxy material properties at room temperature.[19] The moduli and strengths will decrease as the temperature is increased.

A compressive axial load of 140 kips (100 kips times 1.4 safety factor) and a temperature increase of 250 °F were applied to the joint. The resulting deflected shape (greatly exaggerated), axial stress, and shear stress distributions calculated by the COSMOS/M program are shown in figure 11. Similar results for a temperature decrease of 250 °F are given in figure 12. These results are identical, except for a difference in sign, to those that would be obtained with a 140 kip tensile load applied with ±250 °F temperature changes. Figures 11 and 12 indicate that very high stresses will be produced in the joint. Actual stresses would be somewhat smaller since the stress-relieving effects of plastic deformation were not included in the analysis.

From these results, it appears that allowable bond-line shear stresses between the three components of the joint will be exceeded. Also, the ±10° layup graphite/epoxy strut may fail at the tip of its taper. These stresses might possibly be reduced by increasing the length of the joint and making all of the tapers sharper, but it may be impossible to connect a ±10° layup graphite/epoxy strut to an aluminum end fitting in an environment where large temperature changes occur. Differential thermal expansion problems can be reduced by increasing the ply angle from 10°, but, as the ply angle is increased, the advantages of the composite material over that of aluminum soon disappear. A mechanical joint does not appear to be practical because a large number of fasteners would be required, and the ±10° layup is not suitable due to the tear-out failure mode.[19] Controlling the temperature variations in the truss using active cooling may be the only way to keep the composite/aluminum joint from self-destructing.

V. ANALYSIS OF THE JOINT TEMPERATURE DURING WELDING

Advanced space structural concepts is a task initiated to develop assembly methods and welding techniques for in-space joining of structures. The focus is directed toward welding tubular fluid-carrying truss-support struts for a 120-ft diameter aerobrake. The strut is composed of a graphite/epoxy tube with aluminum fittings at the ends of the strut for welding to a mating metallic node (fig. 13).

For the welding process to be effective, the tubes being connected are melted, via a weld torch, and a fusion of the joint is achieved. The temperature at the fusion line is necessarily the melting temperature of the material being joined. As heat is transferred during welding, the temperature of the metallic end fittings, the composite strut, and the metallic node increase. The composite strut is designed to tolerate a maximum temperature of approximately 300 °F. The distance between the weld line and the edge of the composite strut required to avoid thermal damage to the composite strut is estimated in this section.

The welding process selected for this application is GTAW because it is appropriate for welding 1- to 6-in diameter tubes. Here a three-pass weld is required. The first pass will melt and join one half of the thickness. On the second pass, filler wire will be fed into the groove, thereby joining the remainder

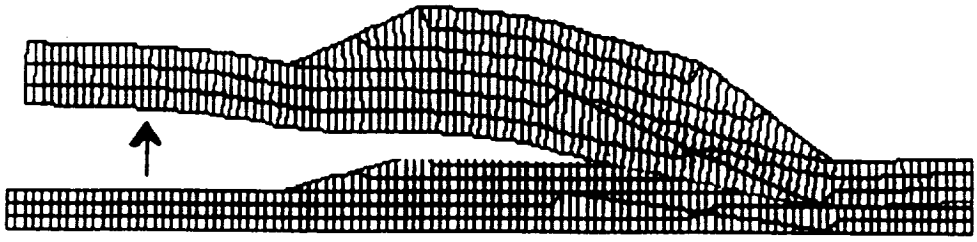

(a) Deflected Shape

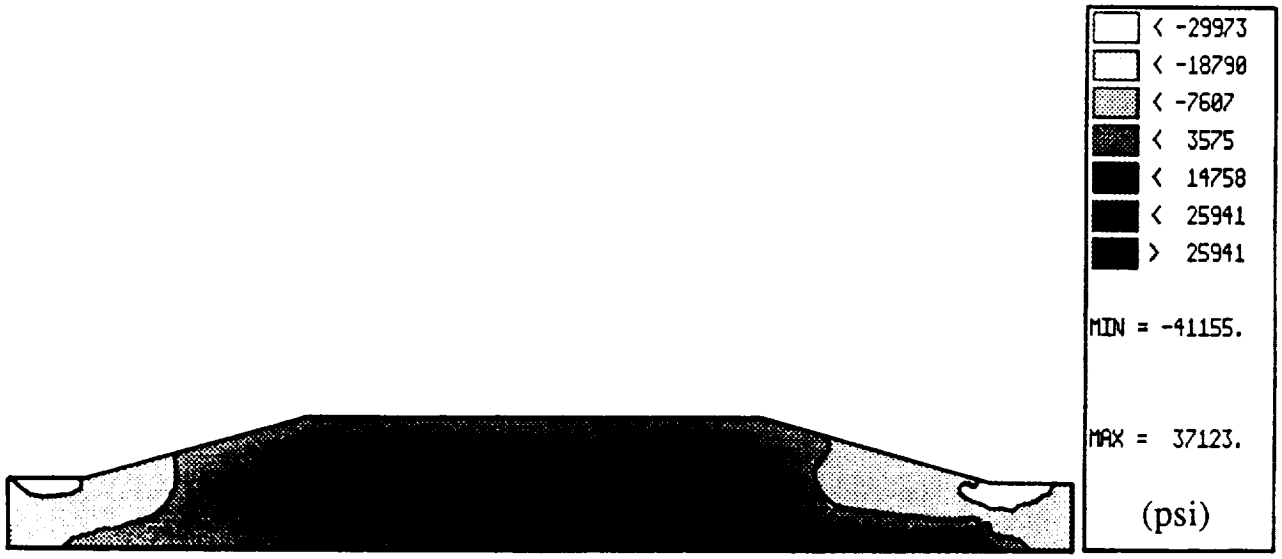

(b) Axial Stress

(c) Shear Stress

Figure 11. Deflection and stresses in the composite material strut-aluminum end fitting joint due to a compressive load of 140 kips and a temperature increase of 250 °F.

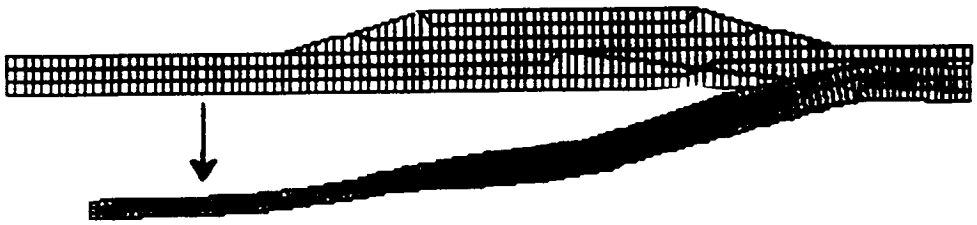

(a) Deflected Shape

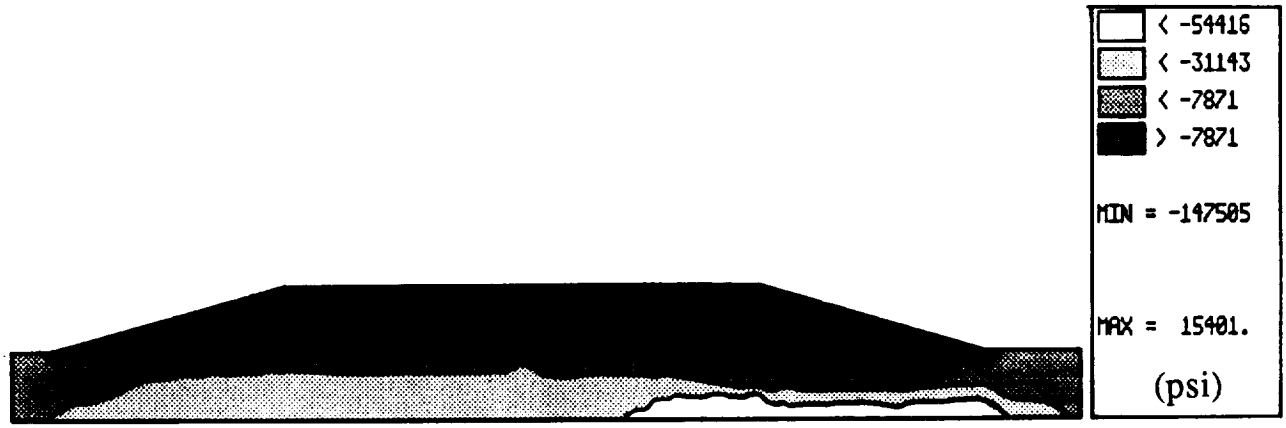

(b) Axial Stress

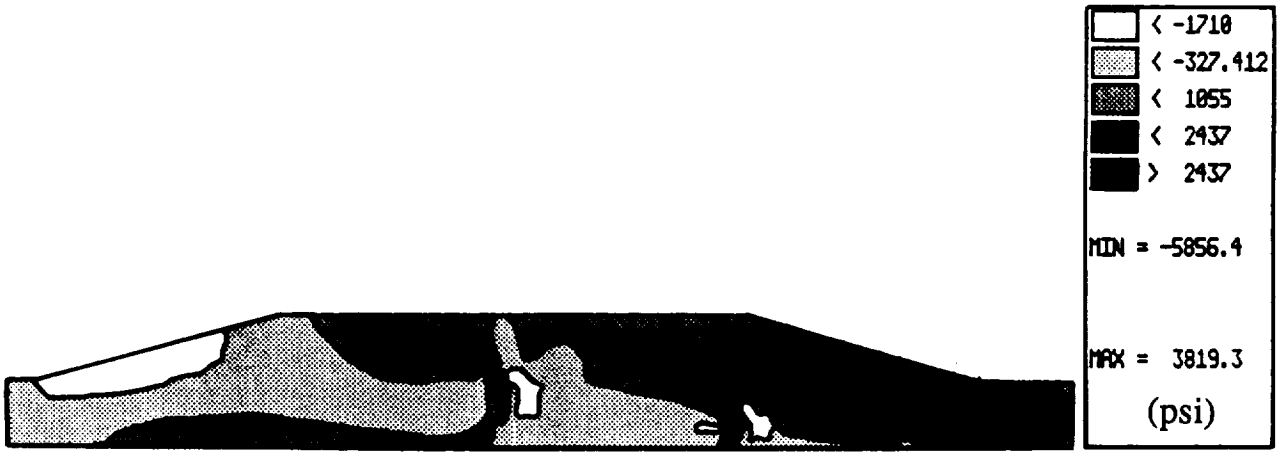

(c) Shear Stress

Figure 12. Deflection and stresses in the composite material strut-aluminum end fitting joint due to a compressive load of 140 kips and a temperature increase of 250 °F.

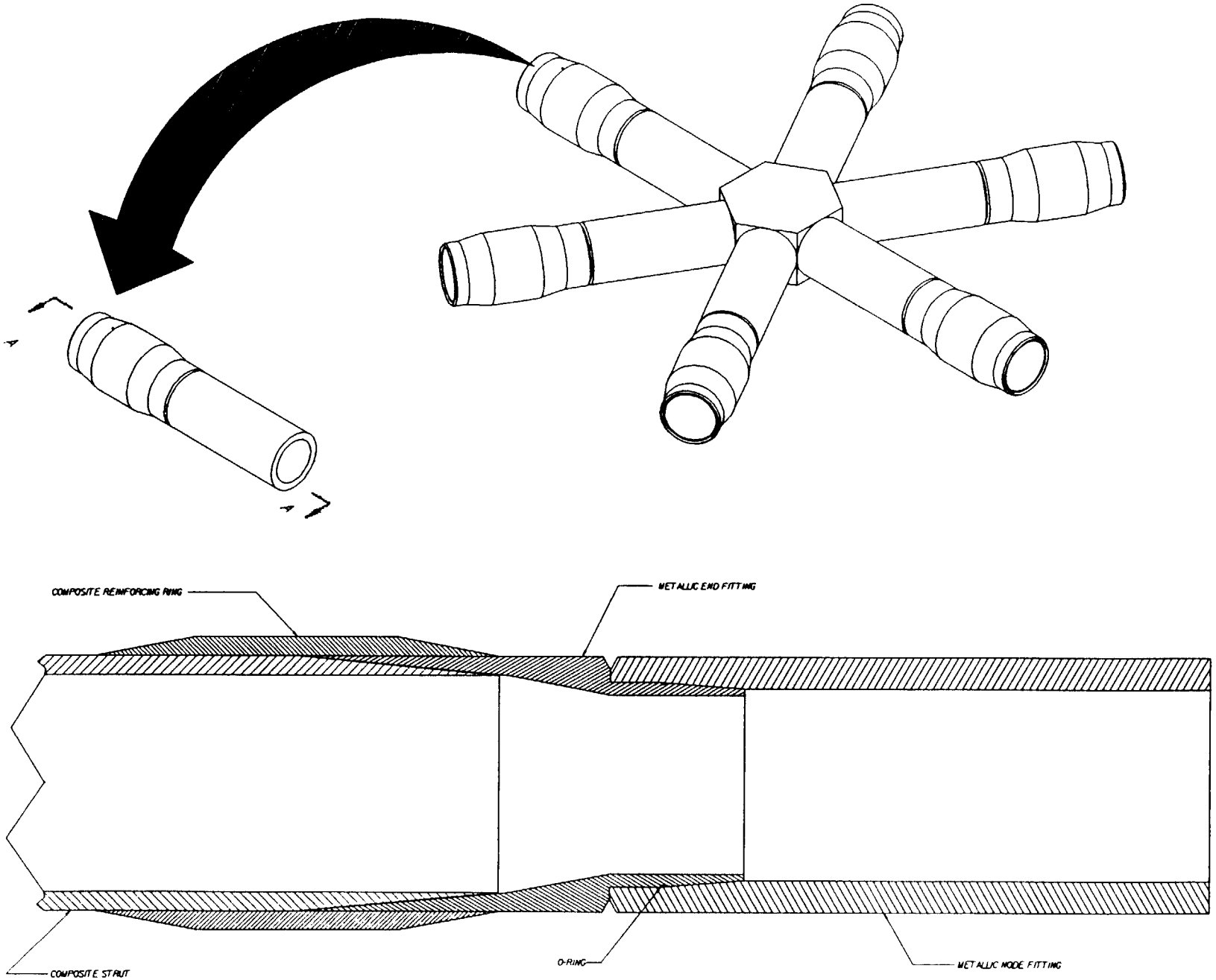

Figure 13. Drawing of a node and a welded joint.

of the tube cross section. A third pass will be made without filler wire to ensure complete fusion of the weld. It was assumed that the initial temperature in the vicinity of the weld will be 32 °F. It was further assumed that after both the first and second passes, the temperature at the fusion line will be allowed to cool to the initial temperature. In this scenario, the area in the vicinity of the weld will be either actively cooled or heated, as required, to a temperature of 32 °F before the beginning of each welding pass. Other parameters affecting the peak temperature at a distance from the fusion line include weld velocity, material melting temperature, and power input. The power input, P (Btu/min), is determined by:[21]

$$P = \frac{-2\pi Kh(T_m - T_o)}{\ln(vd/(4.5\alpha))}, \tag{2}$$

where K = thermal conductivity (0.1625 Btu/(min in °F)), h = thickness of weld material (0.5 in), T_m = melting temperature of 2219 aluminum alloy (1,080 °F), T_o = initial temperature (32 °F), v = welding velocity (10 in/min),[22] d = weld width (0.5 in), ρ = weight density of the aluminum (0.103 lb/in^3), C = specific heat (0.23 Btu/(lb °F)), and α = thermal diffusivity = $K/(\rho C)$ (6.86 in^2/min). Equation (2) predicts a power input of P = 294 Btu/min. The current, either direct or alternating, is dictated by the electrode diameter and American Welding Society classification of tungsten electrode. For most GTAW welding, a 1/16-in diameter EWP classification electrode is used. The amperage for the direct and alternating currents range from 50 to 150 A.[23]

A fundamental entity in the study of heat flow in arc welding is arc energy input, H_{net}, and is defined as the ratio of the effective input power of the heat source to its travel velocity. Not all of the heat generated in the arc can be effectively utilized in arc welding due to heat losses caused by conduction, radiation, and splashing off of droplets (spatter).[24] To account for the heat loss, a heat transfer efficiency term, f_1, is introduced which is the ratio of the heat actually transferred to the workpiece divided by the total heat generated by the heat source.[24] For GTAW, the heat transfer efficiency range is 21 to 48 percent.[24] Thus, $H_{net} = f_1 P/v$.

Having selected the material, thickness, weld velocity, initial temperature, heat transfer efficiency, and welding process, the peak temperature T_p (°F), at a distance y (in), from the fusion line is:[24]

$$T_p = T_o + \left\{ \frac{H_{net}(T_m - T_o)}{[(2\pi e)^{0.5} \rho C h y (T_m - T_o) + H_{net}]} \right\}, \tag{3}$$

where e = 2.718 is the base of natural logarithms. Thus, according to equation (3), the distance the composite components should be from the fusion line to avoid temperatures greater than 300 °F is 0.8 in for the maximum heat transfer efficiency of 48 percent. Intuitively, this distance appears to be too small. However, similar results have recently been obtained experimentally.[21] To be safe, it is recommended that a 2-in spacing be maintained between the fusion line and the edge of a composite material component.

Figure 13 shows an O-ring (silicone elastomer, size AS 568-044)[25] which is intended to provide a frictional force to hold the assembled joint in position during welding. This O-ring may sustain some thermal damage during the welding process without compromising the integrity of the joint. The O-ring serves no function after the welding has been completed.

VI. CONCLUSIONS

On the basis of this study, the following conclusions were reached:

1. Member length errors should be carefully controlled in large truss structures. Member length errors can lock in large stresses and structural distortions before service loads are applied. Distortions may cause problems for instruments with accurate pointing requirements. Distortions may also disturb the flow of hot gases over an aerobrake heat shield.

2. The assembly robot will need to be designed to exert relatively large forces while building the truss structure. The assembly robot will also require an accurate device for ensuring that the member length is correct before welding.

3. The telescoping member and joint overlap with O-ring approach seems to be a workable approach for positioning the truss members before welding. It is important that the joint system be "designed for assembly."

4. A modified GTAW process appears to be a feasible technique for the automated welding of aluminum components on-orbit.

5. A half-inch thick groove weld will be required to carry the design loads. This weld will be made in three passes. The joint weld should be at least 2 inches from the nearest epoxy bond line to avoid thermal damage to the adhesive.

6. A good design for the graphite/epoxy strut-aluminum end fitting joint is difficult to obtain because of the differential thermal expansion problem. The joint investigated in this study may fail under load unless nonlinear behavior produces a significant amount of stress redistribution. Better thermal control of the truss structure (reduce temperature changes) may be required to avoid a joint failure.

REFERENCES

1. Cirillo, W.M., Kaszubowski, M.J., Ayers, J.K., Llewellyn, C.P., Weidman, D.J., and Meredith, B.D.: "Manned Mars Mission Accommodation—Sprint Mission." NASA TM-100598, 1988.

2. Mikulas, M.M., and Dorsey, J.T.: "An Integrated In-Space Construction Facility for the 21st Century." NASA TM-101515, 1988.

3. Walberg, G.D.: "A Review of Aerobraking for Mars Missions." 39th Congress of the International Astronautical Federation, Bangalore, India, paper No. IAF-88-196, 1988.

4. Braun, R.D., and Blersch, D.J.: "Propulsive Options for a Manned Mars Transportation System." AIAA/ASME/SAE/ASEE 25th Joint Propulsion Conference, Monterey, CA, paper No. AIAA-89-2950, 1989.

5. Dorsey, J.T., and Mikulas, M.M.: "Preliminary Design of a Large Tetrahedral Truss/Hexagonal Panel Aerobrake Structural System." 31st Structures, Structural Dynamics, and Materials Conference, Long Beach, CA, AIAA paper No. 90-1050, 1990.

6. Thomson, M.: "Orbital Construction Design Data Book." Astro Aerospace Corporation, Carpinteria, CA, AAC-TN-1160, 1991.

7. Williamsen, J., Thomas, F., Finckenor, J., and Spiegel, B.: "Definition of Large Components Assembled On-Orbit and Robot Compatible Joints." NASA TM100395, 1990.

8. Rhodes, M.D., Will, R.W., and Wise, M.A.: "A Telerobotic System for Automated Assembly of Large Space Structures." NASA TM-101518, 1989.

9. "MSFC Skylab Corollary Experiment System, Mission Evaluation." NASA TM X-64820, 1974.

10. McKannan, E.C., and Poorman, R.M.: "Skylab M551 Melting Experiment." Proceedings of the Third Space Processing Symposium on Skylab Results, vol. 1, 1976, pp. 85–100.

11. Paton, B.: "State-of-Art and Prospects of Development of Aerospace Engineering in the USSR." Conference on Welding in Space and the Construction of Space Vehicles, American Welding Society, 1991, pp. 1–11.

12. Russel, C., Poorman, R., Jones, C., Nunes, A., and Hoffman, D.: "Considerations of Metal Joining Processes for Space Fabrication, Construction, and Repair." Proceedings of the 23rd International SAMPE Technical Conference, Kiamesha Lake, NY, 1991.

13. Mikulas, M.M., Bush, H.G., and Card, M.F.: "Structural Stiffness, Strength, and Dynamic Characteristics of Large Tetrahedral Space Truss Structures." NASA TM X-74001, 1977.

14. "MSC/pal 2 User's Manual." MacNeal-Schwendler Corporation, Los Angeles, CA, 1987.

15. Dorsey, J.T., and Mikulas, M.M.: "Preliminary Design of a Large Tetrahedral Truss/Hexagonal Heatshield Panel Aerobrake." NASA TM 101612, 1989.

16. "Metallic Materials and Elements for Aerospace Vehicle Structures." MIL-HDBK-5D, Department of Defense, Naval Publications and Forms Center, Philadelphia, PA, 1983, pp. 3–152.

17. Saunders, H.L.: "Welding Aluminum: Theory and Practice." The Aluminum Association, 1989, pp. 8.1–8.11.

18. Hoskin, B.C., and Baker, A.A.: "Composite Materials for Aircraft Structures." American Institute of Aeronautics and Astronautics, Inc., New York, NY, 1986, pp. 91 and 120.

19. "Engineered Materials Handbook, Volume 1: Composites." ASM International, Metals Park, OH, 1989, pp. 402,223,479.

20. "COSMOS/M User Guide, Version 1.6." Structural Research and Analysis Corporation, Santa Monica, CA, 1990.

21. Nunes, A., personal communication, 1992.

22. Hoffman, D., personal communication, 1992.

23. "Aluminum Structural Code." Structural Welding Committee, ANSI/AWS D1.2-90, American Welding Society, Miami, FL, 1990, pp. 25–26.

24. "Welding Handbook." Vol. 1, 8th ed., American Welding Society, 1987, pp. 69 and 81–83.

25. "National O-Rings Engineering Manual." Federal-Mogul Corporation, 1982, pp. 28 and 66.

APPENDIX A

Listing of the Nodal Coordinates of the Finite Element Model of the Tetrahedral Truss

NODE ID.	X-COORD.	Y-COORD.	Z-COORD.
1	-31.3900	-54.3800	10.2500
3	-18.8400	-54.3800	10.2500
5	-6.2800	-54.3800	10.2500
7	6.2800	-54.3800	10.2500
9	18.8400	-54.3800	10.2500
11	31.3900	-54.3800	10.2500
31	-37.6700	-43.5000	10.2500
32	-31.3900	-47.1300	0.0000
33	-25.1100	-43.5000	10.2500
34	-18.8400	-47.1300	0.0000
35	-12.5600	-43.5000	10.2500
36	-6.2800	-47.1300	0.0000
37	0.0000	-43.5000	10.2500
38	6.2800	-47.1300	0.0000
39	12.5600	-43.5000	10.2500
40	18.8400	-47.1300	0.0000
41	25.1100	-43.5000	10.2500
42	31.3900	-47.1300	0.0000
43	37.6700	-43.5000	10.2500
61	-43.9500	-32.6300	10.2500
62	-37.6700	-36.2500	0.0000
63	-31.3900	-32.6300	10.2500
64	-25.1100	-36.2500	0.0000
65	-18.8400	-32.6300	10.2500
66	-12.5600	-36.2500	0.0000
67	-6.2800	-32.6300	10.2500
68	0.0000	-36.2500	0.0000
69	6.2800	-32.6300	10.2500
70	12.5600	-36.2500	0.0000
71	18.8400	-32.6300	10.2500
72	25.1100	-36.2500	0.0000
73	31.3900	-32.6300	10.2500
74	37.6700	-36.2500	0.0000
75	43.9500	-32.6300	10.2500
91	-50.2300	-21.7500	10.2500
92	-43.9500	-25.3800	0.0000
93	-37.6700	-21.7500	10.2500
94	-31.3900	-25.3800	0.0000
95	-25.1100	-21.7500	10.2500
96	-18.8400	-25.3800	0.0000
97	-12.5600	-21.7500	10.2500
98	-6.2800	-25.3800	0.0000
99	0.0000	-21.7500	10.2500
100	6.2800	-25.3800	0.0000
101	12.5600	-21.7500	10.2500
102	18.8400	-25.3800	0.0000
103	25.1100	-21.7500	10.2500
104	31.3900	-25.3800	0.0000
105	37.6700	-21.7500	10.2500
106	43.9500	-25.3800	0.0000
107	50.2300	-21.7500	10.2500
121	-56.5100	-10.8800	10.2500
122	-50.2300	-14.5000	0.0000
123	-43.9500	-10.8800	10.2500
124	-37.6700	-14.5000	0.0000
125	-31.3900	-10.8800	10.2500
126	-25.1100	-14.5000	0.0000
127	-18.8400	-10.8800	10.2500
128	-12.5600	-14.5000	0.0000
129	-6.2800	-10.8800	10.2500
130	0.0000	-14.5000	0.0000
131	6.2800	-10.8800	10.2500
132	12.5600	-14.5000	0.0000
133	18.8400	-10.8800	10.2500
134	25.1100	-14.5000	0.0000
135	31.3900	-10.8800	10.2500
136	37.6700	-14.5000	0.0000
137	43.9500	-10.8800	10.2500
138	50.2300	-14.5000	0.0000
139	56.5100	-10.8800	10.2500
151	-62.7900	0.0000	10.2500
152	-56.5100	-3.6300	0.0000
153	-50.2300	0.0000	10.2500
154	-43.9500	-3.6300	0.0000
155	-37.6700	0.0000	10.2500
156	-31.3900	-3.6300	0.0000
157	-25.1100	0.0000	10.2500
158	-18.8400	-3.6300	0.0000
159	-12.5600	0.0000	10.2500
160	-6.2800	-3.6300	0.0000
161	0.0000	0.0000	10.2500
162	6.2800	-3.6300	0.0000
163	12.5600	0.0000	10.2500
164	18.8400	-3.6300	0.0000
165	25.1100	0.0000	10.2500
166	31.3900	-3.6300	0.0000
167	37.6700	0.0000	10.2500
168	43.9500	-3.6300	0.0000
169	50.2300	0.0000	10.2500
170	56.5100	-3.6300	0.0000
171	62.7900	0.0000	10.2500
183	-56.5100	10.8800	10.2500
184	-50.2280	7.2500	0.0000
185	-43.9500	10.8800	10.2500
186	-37.6700	7.2500	0.0000
187	-31.3900	10.8800	10.2500
188	-25.1100	7.2500	0.0000
189	-18.8400	10.8800	10.2500
190	-12.5600	7.2500	0.0000
191	-6.2800	10.8800	10.2500
192	0.0000	7.2500	0.0000
193	6.2800	10.8800	10.2500
194	12.5600	7.2500	0.0000
195	18.8300	10.8800	10.2500
196	25.1100	7.2500	0.0000
197	31.3900	10.8800	10.2500
198	37.6700	7.2500	0.0000
199	43.9500	10.8800	10.2500
200	50.2300	7.2500	0.0000
201	56.5100	10.8800	10.2500
215	-50.2300	21.7500	10.2500
216	-43.9500	18.1300	0.0000
217	-37.6700	21.7500	10.2500
218	-31.3900	18.1300	0.0000
219	-25.1100	21.7500	10.2500
220	-18.8400	18.1300	0.0000
221	-12.5600	21.7500	10.2500
222	-6.2800	18.1300	0.0000
223	0.0000	21.7500	10.2500
224	6.2800	18.1300	0.0000
225	12.5600	21.7500	10.2500
226	18.8400	18.1300	0.0000
227	25.1100	21.7500	10.2500
228	31.3900	18.1300	0.0000
229	37.6700	21.7500	10.2500
230	43.9500	18.1300	0.0000
231	50.2300	21.7500	10.2500
247	-43.9500	32.6300	10.2500
248	-37.6700	29.0000	0.0000
249	-31.3900	32.6300	10.2500
250	-25.1100	29.0000	0.0000
251	-18.8400	32.6300	10.2500
252	-12.5600	29.0000	0.0000
253	-6.2800	32.6300	10.2500
254	0.0000	29.0000	0.0000
255	6.2800	32.6300	10.2500
256	12.5600	29.0000	0.0000
257	18.8400	32.6300	10.2500
258	25.1100	29.0000	0.0000
259	31.3900	32.6300	10.2500
260	37.6700	29.0000	0.0000
261	43.9500	32.6300	10.2500
279	-37.6700	43.5000	10.2500
280	-31.3900	39.8800	0.0000
281	-25.1100	43.5000	10.2500
282	-18.8400	39.8800	0.0000
283	-12.5600	43.5000	10.2500
284	-6.2800	39.8800	0.0000
285	0.0000	43.5000	10.2500
286	6.2800	39.8800	0.0000
287	12.5600	43.5000	10.2500
288	18.8400	39.8800	0.0000
289	25.1100	43.5000	10.2500
290	31.3900	39.8800	0.0000
291	37.6700	43.5000	10.2500
311	-31.3900	54.3800	10.2500
312	-25.1100	50.7500	0.0000
313	-18.8400	54.3800	10.2500
314	-12.5600	50.7500	0.0000
315	-6.2800	54.3800	10.2500
316	0.0000	50.7500	0.0000
317	6.2800	54.3800	10.2500
318	12.5600	50.7500	0.0000
319	18.8400	54.3800	10.2500
320	25.1100	50.7500	0.0000
321	31.3900	54.3800	10.2500

APPENDIX B

Listing of the Nodal Connectivities of the Elements of the Finite Element Model of the Truss

EL. No.	NOD 1	NOD 2
1	31	32
2	32	33
3	33	34
4	34	35
5	35	36
6	36	37
7	37	38
8	38	39
9	39	40
10	40	41
11	41	42
12	42	43
13	61	62
14	62	63
15	63	64
16	64	65
17	65	66
18	66	67
19	67	68
20	68	69
21	69	70
22	70	71
23	71	72
24	72	73
25	73	74
26	74	75
27	91	92
28	92	93
29	93	94
30	94	95
31	95	96
32	96	97
33	97	98
34	98	99
35	99	100
36	100	101
37	101	102
38	102	103
39	103	104
40	104	105
41	105	106
42	106	107
43	121	122
44	122	123
45	123	124
46	124	125
47	125	126
48	126	127
49	127	128
50	128	129
51	129	130
52	130	131
53	131	132
54	132	133
55	133	134
56	134	135
57	135	136
58	136	137
59	137	138
60	138	139
61	151	152
62	152	153
63	153	154
64	154	155
65	155	156
66	156	157
67	157	158
68	158	159
69	159	160
70	160	161
71	161	162
72	162	163
73	163	164
74	164	165
75	165	166
76	166	167
77	167	168
78	168	169
79	169	170
80	170	171
81	183	184
82	184	185
83	185	186
84	186	187
85	187	188
86	188	189
87	189	190
88	190	191
89	191	192
90	192	193
91	193	194
92	194	195
93	195	196
94	196	197
95	197	198
96	198	199
97	199	200
98	200	201
99	215	216
100	216	217
101	217	218
102	218	219
103	219	220
104	220	221
105	221	222
106	222	223
107	223	224
108	224	225
109	225	226
110	226	227
111	227	228
112	228	229
113	229	230
114	230	231
115	247	248
116	248	249
117	249	250
118	250	251
119	251	252
120	252	253
121	253	254
122	254	255
123	255	256
124	256	257
125	257	258
126	258	259
127	259	260
128	260	261
129	279	280
130	280	281
131	281	282
132	282	283
133	283	284
134	284	285
135	285	286
136	286	287
137	287	288
138	288	289
139	289	290
140	290	291
141	311	312
142	312	313
143	313	314
144	314	315
145	315	316
146	316	317
147	317	318
148	318	319
149	319	320
150	320	321
151	1	3
152	3	5
153	5	7
154	7	9
155	9	11
156	31	33
157	33	35
158	35	37
159	37	39
160	39	41
161	41	43
162	61	63
163	63	65
164	65	67
165	67	69
166	69	71
167	71	73
168	73	75
169	91	93
170	93	95
171	95	97
172	97	99
173	99	101
174	101	103
175	103	105
176	105	107
177	121	123
178	123	125
179	125	127
180	127	129
181	129	131
182	131	133
183	133	135
184	135	137
185	137	139
186	151	153
187	153	155
188	155	157
189	157	159
190	159	161
191	161	163
192	163	165
193	165	167
194	167	169
195	169	171
196	183	185
197	185	187
198	187	189
199	189	191
200	191	193
201	193	195
202	195	197
203	197	199
204	199	201
205	215	217
206	217	219
207	219	221
208	221	223
209	223	225
210	225	227
211	227	229
212	229	231
213	247	249
214	249	251
215	251	253
216	253	255
217	255	257
218	257	259
219	259	261
220	279	281
221	281	283
222	283	285
223	285	287
224	287	289
225	289	291
226	311	313
227	313	315
228	315	317
229	317	319
230	319	321
231	32	34
232	34	36
233	36	38
234	38	40
235	40	42
236	62	64
237	64	66
238	66	68
239	68	70
240	70	72
241	72	74
242	92	94
243	94	96
244	96	98
245	98	100
246	100	102
247	102	104
248	104	106
249	122	124
250	124	126
251	126	128
252	128	130
253	130	132
254	132	134
255	134	136
256	136	138
257	152	154
258	154	156
259	156	158
260	158	160
261	160	162
262	162	164
263	164	166
264	168	168
265	168	170
266	184	186
267	186	188
268	188	190
269	190	192
270	192	194
271	194	196
272	196	198
273	198	200
274	216	218
275	218	220
276	220	222
277	222	224
278	224	226
279	226	228
280	228	230
281	248	250
282	250	252
283	252	254
284	254	256
285	256	258
286	258	260
287	280	282
288	282	284
289	284	286
290	286	288
291	288	290
292	312	314
293	314	316
294	316	318
295	318	320
296	1	32
297	3	34
298	5	36
299	7	38
300	9	40
301	11	42
302	31	62
303	33	64
304	35	66
305	37	68
306	39	70
307	41	72
308	43	74
309	61	92
310	63	94
311	65	96
312	67	98
313	69	100
314	71	102
315	73	104
316	75	106
317	91	122
318	93	124
319	95	126
320	97	128
321	99	130
322	101	132
323	103	134
324	105	136
325	107	138
326	121	152
327	123	154
328	125	156
329	127	158
330	129	160
331	131	162
332	133	164
333	135	166
334	137	168
335	139	170
336	153	184
337	155	186
338	157	188
339	159	190
340	161	192
341	163	194
342	165	196
343	167	198
344	169	200
345	185	216
346	187	218
347	189	220
348	191	222
349	193	224
350	195	226
351	197	228
352	199	230
353	217	248
354	219	250
355	221	252
356	223	254
357	225	256
358	227	258
359	229	260
360	249	280
361	251	282
362	253	284
363	255	286
364	257	288
365	259	290
366	281	312
367	283	314
368	285	316
369	287	318
370	289	320
371	1	31
372	31	61
373	61	91
374	91	121
375	121	151
376	3	33
377	33	63
378	63	93
379	93	123
380	123	153
381	153	183
382	5	35
383	35	65
384	65	95
385	95	125
386	125	155
387	155	185
388	185	215
389	7	37
390	37	67
391	67	97
392	97	127
393	127	157
394	157	187
395	187	217
396	217	247
397	9	39
398	39	69
399	69	99
400	99	129
401	129	159
402	159	189
403	189	219
404	219	249
405	249	279
406	11	41
407	41	71
408	71	101
409	101	131
410	131	161
411	161	191
412	191	221
413	221	251
414	251	281
415	281	311
416	43	73
417	73	103
418	103	133
419	133	163
420	163	193
421	193	223
422	223	253
423	253	283
424	283	313
425	75	105
426	105	135
427	135	165
428	165	195
429	195	225
430	225	255
431	255	285
432	285	315
433	107	137
434	137	167
435	167	197
436	197	227
437	227	257
438	257	287
439	287	317
440	139	169
441	169	199
442	199	229
443	229	259
444	259	289
445	289	319
446	171	201
447	201	231
448	231	261
449	261	291
450	291	321
451	32	62
452	62	92
453	92	122
454	122	152
455	34	64
456	64	94
457	94	124
458	124	154
459	154	184
460	36	66
461	66	96
462	96	126
463	126	156
464	156	186
465	186	216
466	38	68
467	68	98
468	98	128
469	128	158
470	158	188
471	188	218
472	218	248
473	40	70
474	70	100
475	100	130
476	130	160
477	160	190
478	190	220
479	220	250
480	250	280
481	42	72
482	72	102
483	102	132
484	132	162
485	162	192
486	192	222
487	222	252
488	252	282
489	282	312
490	74	104
491	104	134
492	134	164
493	164	194
494	194	224
495	224	254
496	254	284
497	284	314
498	106	136
499	136	166
500	166	196
501	196	226
502	226	256
503	256	286
504	286	316
505	138	168
506	168	198
507	198	228
508	228	258
509	258	288
510	288	318
511	170	200
512	200	230
513	230	260
514	260	290
515	290	320
516	11	43
517	43	75
518	75	107
519	107	139
520	139	171
521	9	41
522	41	73
523	73	105
524	105	137
525	137	169
526	169	201
527	7	39
528	39	71
529	71	103
530	103	135
531	135	167
532	167	199
533	199	231
534	5	37
535	37	69
536	69	101
537	101	133
538	133	165
539	165	197
540	197	229
541	229	261
542	3	35
543	35	67
544	67	99
545	99	131
546	131	163
547	163	195
548	195	227
549	227	259
550	259	291
551	1	33
552	33	65
553	65	97
554	97	129
555	129	161
556	161	193
557	193	225
558	225	257
559	257	289
560	289	321
561	31	63
562	63	95
563	95	127
564	127	159
565	159	191
566	191	223
567	223	255
568	255	287
569	287	319
570	61	93
571	93	125
572	125	157
573	157	189
574	189	221
575	221	253
576	253	285
577	285	317
578	91	123
579	123	155
580	155	187
581	187	219
582	219	251
583	251	283
584	283	315
585	121	153
586	153	185
587	185	217
588	217	249
589	249	281
590	281	313
591	151	183
592	183	215
593	215	247
594	247	279
595	279	311
596	42	74
597	74	106
598	106	138
599	138	170
600	40	72
601	72	104
602	104	136
603	136	168
604	168	200
605	38	70
606	70	102
607	102	134
608	134	166
609	166	198
610	198	230
611	36	68
612	68	100
613	100	132
614	132	164
615	164	196
616	196	228
617	228	260
618	34	66
619	66	98
620	98	130
621	130	162
622	162	194
623	194	226
624	226	258
625	258	290
626	32	64
627	64	96
628	96	128
629	128	160
630	160	192
631	192	224
632	224	256
633	256	288
634	288	320
635	62	94
636	94	126
637	126	158
638	158	190
639	190	222
640	222	254
641	254	286
642	286	318
643	92	124
644	124	156
645	156	188
646	188	220
647	220	252
648	252	284
649	284	316
650	122	154
651	154	186
652	186	218
653	218	250
654	250	282
655	282	314
656	152	184
657	184	216
658	216	248
659	248	280
660	280	312

APPENDIX C

Listing of Program CALCMSFT Used to Calculate Nodal Forces Due to Member Misfits

```
CLS
'A unique seed is used for the random number generator for each run so
' different random numbers are generated for each run.
seed% = (32760# * TIMER) / 86400#
RANDOMIZE seed%
'Here the node information file generated by the VIEW2 program is read in.
INPUT "Enter Name of File Containing Node Information: ", filename1$
OPEN filename1$ FOR INPUT AS #1
FOR i% = 1 TO 7
   INPUT #1, dummy$
NEXT i%

numnodes% = 0 'numnodes% stores the number of nodes.
DIM x#(1 TO 1000), y#(1 TO 1000), z#(1 TO 1000) 'x, y, z are nodal coords.
DO WHILE NOT EOF(1)
   numnodes% = numnodes% + 1
   INPUT #1, dummy%, x#(numnodes%), y#(numnodes%), z#(numnodes%)
LOOP
CLOSE #1
'Here the element info file generated by the VIEW2 program is read in.
INPUT "Enter Name of File Containing Element Information: ", filename2$
OPEN filename2$ FOR INPUT AS #1

FOR i% = 1 TO 7
   INPUT #1, dummy$
NEXT i%

numel% = 0 'numel% stores the total number of elements.
'node1%(i) and node2%(i) are the nodes associated with the i-th element.
DIM node1%(1 TO 1000), node2%(1 TO 1000)
DO WHILE NOT EOF(1)
   numel% = numel% + 1
   INPUT #1, dummy%, eltype%, node1%(numel%), node2%(numel%)
LOOP
CLOSE #1

'Member length errors (misfits) are randomly introduced in the members
' that vary between minus MaxLengthError# and plus MaxLengthError#.
INPUT "Enter Magnitude of Maximum Error In Member Length: ", MaxLengthError#
INPUT "Enter Elastic Modulus: ", ElasticModulus#
INPUT "Enter Member Outside Diameter: ", OutsideDia#
INPUT "Enter Member Inside Diameter: ", InsideDia#
area# = (OutsideDia# ^ 2 - InsideDia# ^ 2) * 3.14159265# / 4#

'fx#(i), fy#(i), and fz#(i) store the net force components due to member
' misfits that are to be applied to the i-th node.
DIM fx#(1 TO numnodes%), fy#(1 TO numnodes%), fz#(1 TO numnodes%)

'elforce#(i) is the misfit force in the i-th element.
DIM elforce#(1 TO numel%)
FOR i% = 1 TO numel%
   'delta# is the length error in the i-th element.
   delta# = MaxLengthError# * (-1 + 2 * RND)
   dx# = x#(node2%(i%)) - x#(node1%(i%))
   dy# = y#(node2%(i%)) - y#(node1%(i%))
   dz# = z#(node2%(i%)) - z#(node1%(i%))
   length# = SQR(dx# ^ 2 + dy# ^ 2 + dz# ^ 2)
   ex# = dx# / length#
   ey# = dy# / length#
   ez# = dz# / length#
   force# = ElasticModulus# * area# * delta# / length#
   elforce#(i%) = -force#
   fx#(node1%(i%)) = fx#(node1%(i%)) - force# * ex#
   fy#(node1%(i%)) = fy#(node1%(i%)) - force# * ey#
```

```
   fz#(node1%(i%)) = fz#(node1%(i%)) - force# * ez#
   fx#(node2%(i%)) = fx#(node2%(i%)) + force# * ex#
   fy#(node2%(i%)) = fy#(node2%(i%)) + force# * ey#
   fz#(node2%(i%)) = fz#(node2%(i%)) + force# * ez#
NEXT i%

'The Loading Stub File contains the loading file title
' followed by a blank line. Other info could be put in the stub file if
' desired.
INPUT "Enter Name of Loading Stub File: ", filename3$
OPEN filename3$ FOR INPUT AS #1

'Count number of lines in the stub file.
numlines% = 0
DO WHILE NOT EOF(1)
   LINE INPUT #1, dummy$
   numlines% = numlines% + 1
LOOP

CLOSE #1
OPEN filename3$ FOR INPUT AS #1
DIM LoadingStubFile$(1 TO numlines%)
FOR i% = 1 TO numlines%
   LINE INPUT #1, LoadingStubFile$(i%)
NEXT i%
CLOSE #1

'The Misfit Loading File is the file of member loads that the STAT2
' program reads in. The Misfit Loading File contains the contents of the
' Loading Stub File to which are appended the member misfit nodal loads
' and then some commands required by STAT2.
INPUT "Enter Name of Misfit Loading File: ", filename4$
OPEN filename4$ FOR OUTPUT AS #1
FOR i% = 1 TO numlines%
   PRINT #1, LoadingStubFile$(i%)
NEXT i%

PRINT #1, "FORCES AND MOMENTS APPLIED 0"
FOR i% = 1 TO numnodes%
   'Node 161 was completely fixed so no forces need
   ' be applied to it. Also, no need to print out nodal forces that
   ' are zero.
   IF i% <> 161 THEN
      IF fx#(i%) <> 0# THEN PRINT #1, "FX "; i%; " "; fx#(i%)
      IF fy#(i%) <> 0# THEN PRINT #1, "FY "; i%; " "; fy#(i%)
      IF fz#(i%) <> 0# THEN PRINT #1, "FZ "; i%; " "; fz#(i%)
   END IF
NEXT i%
PRINT #1, " "
PRINT #1, "SOLVE"
PRINT #1, "QUIT"
PRINT #1, "END"
CLOSE #1

'To get the final member forces the initial, misfit member forces must
' be added to to the member forces calculated by STAT2.
INPUT "Enter Name of File for Storing Initial Member Forces: ", filename5$
OPEN filename5$ FOR OUTPUT AS #1
FOR i% = 1 TO numel%
   PRINT #1, elforce#(i%)
NEXT i%

END
```

APPENDIX D

Listing of Program GETFORCE Used to Calculate the Largest Member Force Due to Member Misfits

```
'The Results Data File is created by STAT2. It contains the results
' of a static analysis of the structure.
INPUT "Enter Results Data File: ", filename1$
OPEN filename1$ FOR INPUT AS #1

'Here the Results Data File is searched for the axial forces
' in the members. AxialForce#(i) is the axial force in the i-th
' member. node1%(i) and node2%(i) are the nodes associated with the
' i-th member.
DIM node1%(1 TO 1000), node2%(1 TO 1000), AxialForce#(1 TO 1000)
elnum% = 0
DO WHILE NOT EOF(1)
   INPUT #1, dummy$
   dummy$ = LTRIM$(dummy$)
   IF LEFT$(dummy$, 7) = "ELEMENT" THEN
      IF LEFT$(dummy$, 14) <> "ELEMENT  MAJOR" THEN
         elnum% = elnum% + 1
         node1%(elnum%) = VAL(MID$(dummy$, 49, 6))
         node2%(elnum%) = VAL(MID$(dummy$, 69, 6))
         INPUT #1, dummy$
         dummy$ = LTRIM$(dummy$)
         AxialForce#(elnum%) = VAL(MID$(dummy$, 6, 13))
      END IF
   END IF
LOOP
CLOSE #1

'The initial member forces were determined when calculating the
' member misfit nodal forces.
INPUT "Enter Name of File Storing Initial Member Forces: ", filename2$
OPEN filename2$ FOR INPUT AS #1
FOR i% = 1 TO elnum%
   INPUT #1, elforce#
   AxialForce#(i%) = AxialForce#(i%) + elforce#
NEXT i%
CLOSE #1

'Here the results are sorted to find largest member force magnitude.
MaxForce# = ABS(AxialForce#(1))
FOR i% = 2 TO elnum%
   IF ABS(AxialForce#(i%)) > MaxForce# THEN MaxForce# = ABS(AxialForce#(i%))
NEXT i%
PRINT
PRINT "Largest Force Magnitude: ";
PRINT USING "##.####^^^^"; MaxForce#
PRINT

'The Output Data File stores the member force results.
INPUT "Enter Output Data File: ", filename3$
OPEN filename3$ FOR OUTPUT AS #1
PRINT #1, "Data From File: "; filename1$; "    Date: "; DATE$; "    Time: "; TIME$
PRINT #1, "Largest Force Magnitude: ";
PRINT #1, USING "##.####^^^^"; MaxForce#
FOR i% = 1 TO elnum%
   PRINT #1, USING "####  "; i%; node1%(i%); node2%(i%);
   PRINT #1, USING "##.####^^^^"; AxialForce#(i%)
NEXT i%
END
```

APPENDIX E

Listing of Program GETDISPL Used to Calculate the Relative Displacement Between Nodes 318 and 320 Due to Member Misfits

```
CLS

'The Results Data File is created by STAT2. It contains the results
' of a static analysis of the structure.
INPUT "Enter Results Data File: ", filename1$
OPEN filename1$ FOR INPUT AS #1

'Here the Results Data File is searched for the displacements of nodes
' 318 and 320.

'dx#, dy#, and dz# store the displacements of nodes 318 and 320
NumDisplace% = 2
displace% = 0
DIM dx#(1 TO NumDisplace%), dy#(1 TO NumDisplace%), dz#(1 TO NumDisplace%)
DO WHILE NOT EOF(1)
   INPUT #1, dummy$
   dummy$ = LTRIM$(dummy$)
   IF LEFT$(dummy$, 3) = "318" THEN
      displace% = displace% + 1
      dx#(displace%) = VAL(MID$(dummy$, 4, 12))
      dy#(displace%) = VAL(MID$(dummy$, 16, 12))
      dz#(displace%) = VAL(MID$(dummy$, 28, 12))
   END IF
   IF LEFT$(dummy$, 3) = "320" THEN
      displace% = displace% + 1
      dx#(displace%) = VAL(MID$(dummy$, 4, 12))
      dy#(displace%) = VAL(MID$(dummy$, 16, 12))
      dz#(displace%) = VAL(MID$(dummy$, 28, 12))
   END IF
LOOP
CLOSE #1

NetDisplace# = SQR((dx#(2) - dx#(1)) ^ 2)
PRINT "Net Displacement Nodes 318-320: ";
PRINT USING " ##.####^^^^"; NetDisplace#

END
```

APPENDIX F

Listing of the MSC/pal 2 Input Deck for the Preliminary Design of the Joint

```
TITLE AXISYMMETRIC MODEL 3
NODAL POINT LOCATIONS 3
1,2,0,9 THROUGH 21,1.875,0,5
22,1.875,0,4.8 THROUGH 30,1.875,0,3.2
31,1.875,0,3.1 THROUGH 34,1.875,0,2.8
35,1.875,0,2.6 THROUGH 40,1.875,0,1.6
41,1.875,0,1.2 THROUGH 44,1.875,0,0
45,2.0625,0,9 THROUGH 65,2,0,5
66,2,0,4.8 THROUGH 74,2,0,3.2
75,2,0,3.1 THROUGH 78,2,0,2.8
79,2,0,2.6 THROUGH 82,2,0,2
83,2.125,0,9 THROUGH 112,2.125,0,3.2
113,2.125,0,3.1 THROUGH 116,2.125,0,2.8
117,2.125,0,2.6 THROUGH 119,2.125,0,2.2
120,2.125,0,2 THROUGH 130,2,0,0
131,2,0,-0.333 THROUGH 133,2,0,-1
134,2.3125,0,9 THROUGH 154,2.1875,0,5
155,2.1875,0,4.8 THROUGH 159,2.25,0,4
160,2.25,0,3.8 THROUGH 163,2.25,0,3.2
164,2.25,0,3.1 THROUGH 167,2.25,0,2.8
168,2.25,0,2.6 THROUGH 170,2.25,0,2.2
171,2.25,0,2 THROUGH 181,2.1563,0,0
182,2.1563,0,-0.333 THROUGH 184,2.1563,0,-1
185,2.5,0,9 THROUGH 205,2.25,0,5
206,2.25,0,4.8 THROUGH 210,2.375,0,4
211,2.375,0,3.8 THROUGH 214,2.375,0,3.2
215,2.375,0,3.1 THROUGH 218,2.375,0,2.8
219,2.375,0,2.6 THROUGH 221,2.375,0,2.2
222,2.375,0,2 THROUGH 232,2.3125,0,0
233,2.3125,0,-0.333 THROUGH 235,2.3125,0,-1
236,2.5625,0,9 THROUGH 256,2.4375,0,5
257,2.4375,0,4.8 THROUGH 261,2.5,0,4
262,2.5,0,3.8 THROUGH 265,2.5,0,3.2
266,2.5,0,3.1 THROUGH 269,2.5,0,2.8
270,2.5,0,2.6 THROUGH 272,2.5,0,2.2
273,2.5,0,2 THROUGH 283,2.4687,0,0
284,2.4687,0,-0.333 THROUGH 286,2.4687,0,-1
287,2.625,0,9 THROUGH 316,2.625,0,3.2
317,2.625,0,3.1 THROUGH 320,2.625,0,2.8
321,2.625,0,2.6 THROUGH 334,2.625,0,0
335,2.625,0,-0.333 THROUGH 337,2.625,0,-1
338,2.825,0,0 THROUGH 341,2.825,0,-1
342,3.025,0,0 THROUGH 345,3.025,0,-1
346,3.225,0,0 THROUGH 349,3.225,0,-1
350,3.425,0,0 THROUGH 353,3.425,0,-1
354,3.625,0,0 THROUGH 357,3.625,0,-1
358,4,0,0 THROUGH 361,4,0,-1
362,4.5,0,0 THROUGH 365,4.5,0,-1
366,5,0,0 THROUGH 369,5,0,-1
370,5.5,0,0 THROUGH 373,5.5,0,-1
374,2.6452,0,0.8
375,2.7085,0,0.6
376,2.825,0,0.4
377,3.025,0,0.2
378,3.225,0,0.0835
379,3.425,0,.0202
380,2.825,0,0.2
381,2.115,0,2.9
382,2.115,0,2.8 THROUGH 385,2.115,0,2.2
386,2.115,0,2 THROUGH 388,2.090,0,1.6
389,2.065,0,1.2 THROUGH 392,1.99,0,0
393,2.125,0,9.4
394,2.125,0,9.2
395,2.3125,0,9.4
396,2.3125,0,9.2
397,2.5,0,9.4
398,2.5,0,9.2

MATERIAL 1.05E+07, 0, 0, .33, 51000, .0000119, 70
QUAD 4 0
ELEMENT GENERATE 21
1 38 82 1 44
45 76 114 1 38
77 82 386 1 304
39 44 392 1 348
103 133 235 1 51
185 235 337 1 51
334 337 373 1 4

CONNECT 76 TO 77 TO 381 TO 114
CONNECT 330 TO 331 TO 375 TO 374
CONNECT 331 TO 332 TO 376 TO 375
CONNECT 332 TO 333 TO 380 TO 376
CONNECT 333 TO 334 TO 338 TO 380
CONNECT 380 TO 338 TO 342 TO 377
CONNECT 377 TO 342 TO 346 TO 378
CONNECT 378 TO 346 TO 350 TO 379
TRIANGLE PLATE TYPE 4,0
CONNECT 38 TO 39 TO 82
CONNECT 82 TO 39 TO 387
CONNECT 82 TO 387 TO 386
CONNECT 329 TO 330 TO 374
CONNECT 376 TO 380 TO 377
CONNECT 379 TO 350 TO 354
MATERIAL 2.32E+07,0, 0, .33, 48000,-2.5E-6, 70
QUAD 4 0
ELEMENT GENERATE 21
83 103 205 1 51

CONNECT 393 TO 394 TO 396 TO 395
CONNECT 394 TO 83 TO 134 TO 396
CONNECT 395 TO 396 TO 398 TO 397
CONNECT 396 TO 134 TO 185 TO 398

ZERO 1
RA ALL
TA 370,371,372,373

END DEF
```

APPENDIX G

Listing of the COSMOS/M Input Deck for the Analysis of the Composite Material-Aluminum Interface Joint

```
EG,1,PLANE2D,0, ,1
EX,1,10.5E6
NUXY,1,0.33
ALPX,1,12E-6
ACTIVE,MAT,1
RC,1,1
ACTIVE,REAL,1
PT,1, , , ,2.125,8,0
PT,2, , , ,2.125,-6,0
PT,3, , , ,2.875,-6,0
PT,4, , , ,2.875,8,0
REGSIZE,113,7,2
AREA,1,1,2,3,4
EDELETE,337,368
EDELETE,449,488
EDELETE,561,608
EDELETE,433,448
EDELETE,537,560
EDELETE,641,672
NDELETE,453,484
NDELETE,566,605
NDELETE,679,726
NDELETE,550,565
NDELETE,655,678
NDELETE,760,791
EX,2,24E6
EY,2,1.7E6
EZ,2,1.7E6
NUXY,2,0.3
NUXZ,2,0.3
NUYZ,2,0.3
GXY,2,0.65E6
ALPX,2,-1.0E-6
ALPY,2,63E-6
ALPZ,2,61E-6
ACTIVE,MAT,2
EMOD,1
EMOD,113
EMODIFY,225
EMODGEN,95, ,1, , ,1
EMODGEN,79, ,113, , ,1
EMODGEN,63, ,225, , ,1
EX,3,2.4E6
EY,3,1.7E6
EZ,3,2.4E6
NUXY,3,0.3
NUXZ,3,0.3
NUYZ,3,0.3
GXY,3,0.65E6
ALPX,3,31E-6
ALPY,3,63E-6
ALPZ,3,31E-6
ACTIVE,MAT,3
EMOD,369
EMODGEN,271, ,369, , ,1
EDELETE,369,369
EDELETE,489,489
EDELETE,609,609
EDELETE,640,640
EDELETE,536,536
EDELETE,432,432
EDELETE,289,289
EDELETE,193,193
EDELETE,96,96
ACTIVE,MAT,3
E,369,372,373,486,486
E,489,493,494,607,607
E,609,728,614,615,615
E,640,646,758,645,645
E,536,540,541,653,653
E,432,435,436,548,548
ACTIVE,MAT,2
E,289,291,292,404,404
E,193,194,195,307,307
E,96,96,97,209,209
ACTIVE,MAT,1
E,675,405,404,292,292
E,674,308,307,195,195
E,673,210,209,97,97
NDELETE,485,485
NDELETE,606,606
NDELETE,727,727
NDELETE,759,759
NDELETE,654,654
NDELETE,549,549
N, 486 , 2.5234375 , 3.875 , 0
N, 487 , 2.546875 , 3.75 , 0
N, 488 , 2.5703125 , 3.625 , 0
N, 489 , 2.59375 , 3.5 , 0
N, 490 , 2.6171875 , 3.375 , 0
N, 491 , 2.640625 , 3.25 , 0
N, 492 , 2.6640625 , 3.125 , 0
N, 493 , 2.6875 , 3 , 0
N,494,2.6875,2.875,0
N, 607 , 2.7109375 , 2.875 , 0
N, 608 , 2.734375 , 2.75 , 0
N, 609 , 2.7578125 , 2.625 , 0
N, 610 , 2.78125 , 2.5 , 0
N, 611 , 2.8046875 , 2.375 , 0
N, 612 , 2.828125 , 2.25 , 0
N, 613 , 2.8515625 , 2.125 , 0
N, 614 , 2.875 , 2 , 0
N, 646 , 2.875 ,-2 , 0
N, 647 , 2.8515625 ,-2.125 , 0
N, 648 , 2.828125 ,-2.25 , 0
N, 649 , 2.8046875 ,-2.375 , 0
N, 650 , 2.78125 ,-2.5 , 0
N, 651 , 2.7578125 ,-2.625 , 0
N, 652 , 2.734375 ,-2.75 , 0
N, 653 , 2.7109375 ,-2.875 , 0
N,540,2.6875,-2.875,0
N, 541 , 2.6875 ,-3 , 0
N, 542 , 2.6640625 ,-3.125 , 0
N, 543 , 2.640625 ,-3.25 , 0
N, 544 , 2.6171875 ,-3.375 , 0
N, 545 , 2.59375 ,-3.5 , 0
N, 546 , 2.5703125 ,-3.625 , 0
N, 547 , 2.546875 ,-3.75 , 0
N, 548 , 2.5234375 ,-3.875 , 0
N,291,2.488281,0,0
N, 292 , 2.48828125 ,-.125 , 0
N, 293 , 2.4765625 ,-.25 , 0
N, 294 , 2.46484375 ,-.375 , 0
N, 295 , 2.453125 ,-.5 , 0
N, 296 , 2.44140625 ,-.625 , 0
N, 297 , 2.4296875 ,-.75 , 0
N, 298 , 2.41796875 ,-.875 , 0
N, 299 , 2.40625 ,-1 , 0
N, 300 , 2.39453125 ,-1.125 , 0
N, 301 , 2.3828125 ,-1.25 , 0
N, 302 , 2.37109375 ,-1.375 , 0
N, 303 , 2.359375 ,-1.5 , 0
N, 304 , 2.34765625 ,-1.625 , 0
N, 305 , 2.3359375 ,-1.75 , 0
N, 306 , 2.32421875 ,-1.875 , 0
N, 307 , 2.3125 ,-2 , 0
N,308,2.3125,-2.125,0
N,194,2.300781,-2,0
N, 195 , 2.30078125 ,-2.125 , 0
N, 196 , 2.2890625 ,-2.25 , 0
N, 197 , 2.27734375 ,-2.375 , 0
N, 198 , 2.265625 ,-2.5 , 0
N, 199 , 2.25390625 ,-2.625 , 0
N, 200 , 2.2421875 ,-2.75 , 0
N, 201 , 2.23046875 ,-2.875 , 0
N, 202 , 2.21875 ,-3 , 0
N, 203 , 2.20703125 ,-3.125 , 0
N, 204 , 2.1953125 ,-3.25 , 0
N, 205 , 2.18359375 ,-3.375 , 0
N, 206 , 2.171875 ,-3.5 , 0
N, 207 , 2.16015625 ,-3.625 , 0
N, 208 , 2.1484375 ,-3.75 , 0
N, 209 , 2.13671875 ,-3.875 , 0
D,1,UZ,0,758, ,ROTX,ROTY,ROTZ
D,113,UY,0,452,113
EP,1,4,26E3,225,112
NT,1,TEMP,250,758
RENUMBER,ON
```

APPROVAL

DESIGN OF A WELDED JOINT FOR ROBOTIC, ON-ORBIT ASSEMBLY OF SPACE TRUSSES

By W.K. Rule and F.P. Thomas

The information in this report has been reviewed for technical content. Review of any information concerning Department of Defense or nuclear energy activities or programs has been made by the MSFC Security Classification Officer. This report, in its entirety, has been determined to be unclassified.

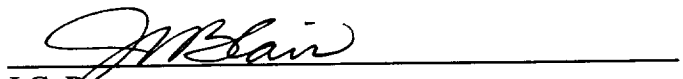

J.C. BLAIR
Director, Structures and Dynamics Laboratory

☆ U.S. GOVERNMENT PRINTING OFFICE 1992—733-050/60210